

Reaction of ClONO₂ with H₂O and HCl in Sulfuric Acid and HNO₃/H₂SO₄/H₂O Mixtures

David R. Hanson

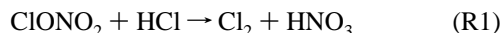
CIRES and NOAA Aeronomy Laboratory, Boulder, Colorado 80303-3328

Received: August 26, 1997; In Final Form: April 13, 1998

Measurements of the reaction probabilities (γ) for ClONO₂ onto sulfuric acid solutions at 200–270 K are described. ClONO₂ uptake due to reaction with H₂O and with HCl in H₂SO₄ solutions (45–55 wt %) was investigated at 203–205 K. ClONO₂ hydrolysis was also investigated on 36.5, 40, and 75 wt % sulfuric acid solutions over a range of temperatures. The measured γ are generally in good agreement with previously reported values. In addition, the solubility of HCl was determined for 45 and 50 wt % sulfuric acid from 200 to 225 K. The uptake of ClONO₂ onto small sulfuric acid particles was studied resulting in a lower limit to the sticking coefficient of 0.5. ClONO₂ reaction probabilities were also measured on H₂SO₄ solutions containing significant amounts of HNO₃. In opposition to previous reports, HNO₃ was found to have a significant effect on γ for ClONO₂: it is as low as one-half of that expected for the comparable HNO₃-free solutions. The measured γ on sulfuric acid solutions at 203 ± 2 K are discussed in terms of solubility, diffusivity, and bulk and surface reactions. Within this framework, the measured γ were fit as a function of H₂SO₄ and HCl content, thus allowing for the measurements to be extrapolated to atmospheric conditions.

Introduction

An important heterogeneous reaction in the high latitude lower stratosphere is¹



In the laboratory, this reaction has been shown to readily occur on many types of materials found in the cold stratosphere, including supercooled sulfuric acid.^{2–8} In previous work from this laboratory,² R1 was measured as a function of partial pressure of HCl, p_{HCl} , at 203 K on sulfuric acid solutions representative of the lower cold stratosphere. These measurements covered the range of typical [HCl] for liquid H₂SO₄ particles in the atmosphere. Zhang et al.⁶ and Elrod et al.⁷ conducted similar measurements and reported that their values for γ for R1 (γ_{R1}) were in good agreement with those of Hanson and Ravishankara.² Furthermore, Ravishankara and Hanson⁹ concluded that liquid droplets, supercooled to near the ice frost point, could facilitate R1 more efficiently than would other Type I polar stratospheric cloud particles such as nitric acid trihydrate or sulfuric acid tetrahydrate.

Recent work on the thermodynamics of sulfuric acid solutions^{10,11} has resulted in water activities, and HCl and HNO₃ solubilities, that can be used to predict the H₂O, HCl, and HNO₃ contents of supercooled sulfuric acid in the stratosphere. The values of some of these quantities, in particular the water activity and HCl solubility in solutions containing ≤ 50 wt % H₂SO₄, are significantly different than what was used by Hanson and Ravishankara;² thus, changes in the rate parameters for R1 are expected. Also, it has been shown^{12–14} that sulfuric acid solutions, when cooled to temperatures near the frost point, take up a large amount of nitric acid. The reaction probabilities for ClONO₂ have been reported^{5–7} to be not significantly affected by the presence of dissolved HNO₃.

Robinson et al.⁸ report γ for the hydrolysis of ClONO₂



on sulfuric acid over a range of temperature and H₂SO₄ content. They presented an analysis of the γ_{R2} data based on the well-known equation¹⁵

$$\frac{1}{\gamma} = \frac{1}{\alpha} + \frac{\omega}{4RTH\sqrt{kD_1}} \quad (3)$$

where α is the mass accommodation coefficient, ω is the mean thermal speed, H is the Henry's law coefficient, k is the loss rate coefficient in the liquid, and D_1 is the liquid-phase diffusion coefficient. Further measurements of γ for ClONO₂ hydrolysis over a range of temperatures and H₂SO₄ contents are needed to test their formulation.

New measurements of R1 and of the hydrolysis of ClONO₂ (R2) are reported here. γ as a function of HCl content was measured for 45, 49.5, 51, 53, and 55 wt % H₂SO₄. Measurements of γ_{R1} and γ_{R2} on HNO₃/H₂SO₄/H₂O solutions are also reported. Measurements of the Henry's law coefficient for HCl (H^*_{HCl}) in sulfuric acid solutions and mixed nitric/sulfuric acid solutions were also performed.

Ravishankara and Hanson⁹ noted that the value of the mass accommodation coefficient (α) for ClONO₂ is uncertain but is likely to be close to unity rather than 0.3, a value that was chosen arbitrarily.² A related parameter is the sticking coefficient S ,¹⁶ the fraction of collisions with the surface that result in accommodation on the surface. Reported here are measurements on aerosol particles containing 49 wt % H₂SO₄ and ~10⁻² M HCl in order to determine S (and/or α) for ClONO₂.

Experimental Section

Bulk Experiment. Reaction probabilities on bulk liquids were measured in a rotating wetted-wall (RWW) flow reactor described by Lovejoy et al.¹⁷ and Hanson and Lovejoy¹⁸ using the procedures described in Hanson and Ravishankara;² only

the significant changes in the bulk experimental technique are described in detail here. Detection of reactants and products was accomplished with a chemical ionization mass spectrometer (CIMS) as described previously.^{2,4,19,20} The solution H₂SO₄ contents investigated were the following: for R1 and R2, 45, 49.5, 51, 53, and 55 wt % at 203–205 K; for R2 only, 75 wt % from 200 to 270 K and 36.5, 41, and 45 wt % at 203 and 230 K. Water vapor was added to the He carrier gas to match the H₂O vapor pressure of the solutions.^{10,21}

A few different RWWs were used in this work, and the inner diameters ranged from 1.85 to 1.90 cm. Standard analysis procedures²² were used to extract values for γ from the measured first-order loss rate coefficients. The small glass-encapsulated “stirring” bar¹⁸ in the RWW or the glass rod applicator² were not used in these experiments because they are a possible source of systematic error. These glass rods (0.4–0.8 mm o.d.) rest on the flow tube wall in the measurement region and compromise the cylindrical symmetry of the flow tube. This could appreciably affect the extracted γ s when gas-phase diffusion significantly affects the measured loss rates²² (i.e., when γ is > 0.05 for typical conditions).

For the measurements of γ_{R1} , HCl was doped into the 49.5, 51, 53, and 55 wt % solutions from the gas phase. HCl introduced with the carrier gas is taken up by the liquid in the RWW until saturation is achieved.¹⁸ Saturation of the solutions was ensured by comparing the HCl entering the flow tube to the HCl in the carrier gas after it passed over the liquid. At 203 K, the time needed to ensure saturation of the solutions is very long for the 49.5 and 51 wt % solutions; thus, HCl vapor was added to these solutions at 230 to 250 K (where H^*_{HCl} is 0.05 to 0.01 times that at 203 K¹⁰.) The RWW was then cooled to 203 K where reactive uptake of ClONO₂ was measured. At all times, water vapor in the He carrier gas was set to match the H₂O vapor pressure of the solutions.^{10,21}

For 45 wt % H₂SO₄, HCl was added by mixing pure 45 wt % H₂SO₄ with small amounts of 45 wt % H₂SO₄ solutions that contained known amounts of HCl.²³ The 50 wt % H₂SO₄ and the HNO₃/H₂SO₄ solutions were prepared in a similar manner, and the solution [HNO₃], [H₂SO₄], and [HCl] were determined from the mixing stoichiometry. The solution densities were taken from the Carslaw et al.¹⁰ model for the H₂SO₄/H₂O solutions and densities of 1.44–1.30 g cm⁻³ were used for the HNO₃/H₂SO₄/H₂O solutions. The solutions were kept cool to minimize evaporation of HCl or HNO₃ during mixing; HCl was added to solutions that were cooled to ~ 273 K (H^*_{HCl} is $> 10^3$ M atm⁻¹).

HCl solubilities in 45 and 50 wt % sulfuric acid solutions were determined by measuring the partial pressure of HCl (p_{HCl}) over solutions containing 10⁻² to 10⁻³ M HCl located in the RWW. The HCl concentration in the sulfuric acid solutions was determined from the mixing stoichiometry as described above. A flow of He (1.5–4 STP cm³ s⁻¹ at ~ 0.4 –7 Torr; volume flow rate of 150–2500 cm³ s⁻¹) over the solution saturates with HCl at the p_{HCl} of the solution²⁴ and p_{HCl} was determined using the CIMS (see below).

Particle Experimental Procedure. The experimental procedure was essentially the same as described previously.^{18,25} The H₂SO₄ content of the conditioner was 49.5 wt %, and the temperature was 240 K. Total pressure (N₂) in the particle flow tube was typically 160 Torr, and the average flow velocity was 6 cm s⁻¹. The distribution of particle sizes is well-described by a log-normal distribution;²⁵ r_p was ~ 0.07 μ m, $\log \sigma \sim 0.1$, and number density $\sim 3 \times 10^5$ cm⁻³. γ_{R1} was studied by doping the aerosol with HCl vapor. This was accomplished by flowing

a small amount of a dilute HCl-in-N₂ mixture into the aerosol flow downstream of the conditioner. p_{HCl} was determined using the CIMS signals, and with $H^*_{HCl} = 8.7 \times 10^4$ M atm⁻¹,¹⁰ [HCl] = $p_{HCl}H^*_{HCl}$ in the particles can be calculated. The conditioner was slightly warmer (0.5–1 K) than the flow tube which leads to excess water vapor; however, there is also a drying effect due to the small flows that do not contain H₂O vapor. The combination of these effects results in aerosol particles of ~ 49 wt % H₂SO₄ (estimated to be known to ± 1 wt %.) The diffusion coefficient of ClONO₂ in N₂ was calculated²⁶ to be 68.2(1 Torr/ p_{N_2})($T/273$ K)^{1.93} cm² s⁻¹.

CIMS and HCl Calibration. The CIMS is described by Lovejoy,²⁷ Huey et al.,²⁰ and Hanson and Ravishankara.¹⁹ The SF₆⁻ reactant ion was primarily used to detect the species ClONO₂, HOCl, HNO₃, and HCl as FCINO₃⁻, SF₅O⁻, FHNO₃⁻, and SF₅Cl⁻ (or FHCl⁻), respectively.^{19,20} The HCl calibration procedure is essentially the same as employed previously in this laboratory.^{2,18,24} The procedure is described in detail here because of the importance of accurately determining p_{HCl} .

The partial pressure of HCl (p_{HCl} , atm) in the RWW is related to the HCl signal (S_{162} , the SF₅³⁵Cl⁻ ion) in the CIMS via the equation

$$p_{HCl} = \frac{S_{162}}{S_{146}} C_{162} \frac{V_F}{L_0} \frac{p_{RWW}}{F} \quad (4)$$

where C_{162} is a constant determined from calibrations (see below), S_{146} and S_{162} are the signals due to the SF₆⁻ reactant ion and the SF₅³⁵Cl⁻ product ion, respectively, V_F is the volume flow rate in the CIMS (cm³ s⁻¹), L_0 is Loschmidt's number (2.69×10^{19} molecule cm⁻³ for STP), p_{RWW} is the total pressure in the RWW (atm), and F is the total gas flow rate in the RWW (STP cm³ s⁻¹). Note that $S_{162} \ll S_{146}$ in these experiments.

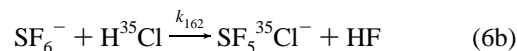
Calibrations for HCl were performed by introducing a known flow of HCl into the CIMS and monitoring the CIMS signals. HCl from a 1.0% HCl in N₂ mixture was used, and thus, the HCl flow rate, F_{HCl} (STP cm³ s⁻¹), was taken to be 0.010 times the total flow rate of the mixture (F_{N_2+HCl} ranged from 10⁻³ to 10⁻² STP cm³ s⁻¹, determined by measuring dP/dt in a known volume). The calibration constant for the CIMS is given by

$$C_{162} = F_{HCl} \frac{S'_{146}}{S'_{162}} \frac{L_0}{V_F^2} \quad (5)$$

where S'_{146} and S'_{162} are the CIMS signals due to the reactant ion and due to HCl (at 162 amu), respectively, during the HCl calibration. The calibration constant for the CIMS is related to the average ion–molecule reaction time, t ,²⁸

$$C_{162} = \frac{1}{tk_{162}V_F} \quad (6a)$$

(assuming very little mass discrimination between 146 and 162 amu). k_{162} is the ion–molecule rate coefficient for



C_{162} is usually determined (eq 5) for each set of measurements. It varies on the order of 10–20% day-to-day (a range of $\pm 25\%$ encompasses the variation on a longer time scale). The uncertainty of the calibration is believed to be $\pm 25\%$. The uncertainty in the measured p_{HCl} can be greater than this especially for low p_{HCl} because of possible small sources of

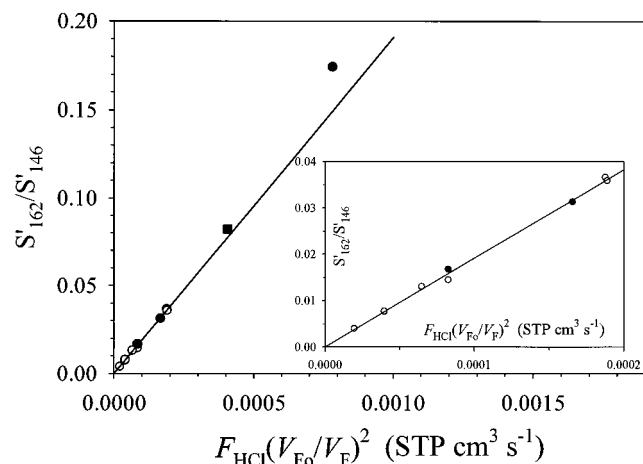


Figure 1. Plot of signal due to HCl (divided by reactant ion signal) versus “normalized” flow rate of HCl. Inset is the lowest flow rate data on enlarged axis. Open symbols, $V_F = V_{F0}$; filled, $V_F < V_{F0}$.

“impurity” HCl (i.e., HCl desorbing from surfaces between the liquid in the RWW and the CIMS).

The calibration constant is related to the dimensions of the CIMS flow tube. Assuming perfect mixing of the HCl flow with the CIMS flow, the average ion–molecule reaction time is given by^{20,28}

$$t = \frac{t_{\text{plug}}}{1.6} = \frac{zA}{1.6V_F} \quad (7)$$

where t_{plug} is the reaction time assuming plug flow, z is the distance between the injection point of HCl and the sampling orifice into the mass spectrometer, and A is the cross sectional area of the CIMS flow tube. Then C_{162} is given by

$$C_{162} = \frac{1.6}{zAk_{162}} \quad (8)$$

Calibrations for HCl provide a measure of the average ion–molecule reaction time, t (eq 7). Note that the CIMS sensitivities for other molecules of interest can be estimated using t determined from a calibration and eq 6a provided the ion–molecule rate coefficients are known. This was done to provide rough calibrations of the CIMS for ClONO₂ and HNO₃, using the rate coefficients and product yields of Huey et al.²⁰ Note that if the product ion is very different in mass from the product ion of the calibrated species, this estimate could be influenced by possible mass discrimination effects in the CIMS. Also note that t or z determined in a calibration may be sensitive to how well the reactant mixes with the ions in the CIMS. Calibrations were performed by introducing F_{HCl} with the flow from the neutral flow tube under typical experimental conditions.

The ion–molecule reaction



was used to monitor $p_{\text{H}_2\text{O}}$ over some of the HNO₃/H₂SO₄/H₂O solutions. This was done to check for a change in $p_{\text{H}_2\text{O}}$ when the solutions froze. Absolute $p_{\text{H}_2\text{O}}$ were not determined.

A plot of S'_{162}/S'_{146} vs $F_{\text{HCl}}(V_{F0}/V_F)^2$, i.e., a “normalized” HCl flow rate, is shown in Figure 1 ($V_{F0} = 2.8 \times 10^5 \text{ cm}^3 \text{ s}^{-1}$ is the typical volume flow rate in the CIMS flow tube). F_{HCl} was varied from 10^{-5} to 10^{-4} STP $\text{cm}^3 \text{ s}^{-1}$, and V_F was $(1.3\text{--}2.8) \times 10^5 \text{ cm}^3 \text{ s}^{-1}$. Excellent linearity is demonstrated, and the slope of a linear regression to the data is related to C_{162} via

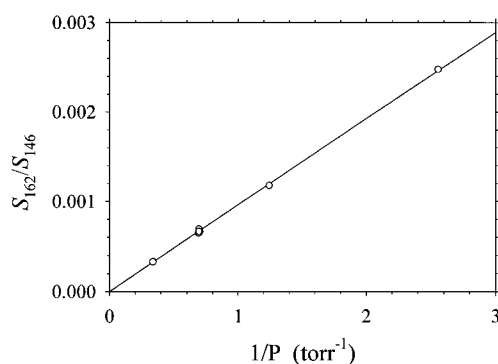


Figure 2. Plot of signal due to HCl (divided by reactant ion signal) versus inverse total pressure in the RWW. The x -axis is a proxy for volume flow rate in the RWW. The line is a linear regression forced through zero.

TABLE 1: H^*_{HCl} Measured Here

wt % H ₂ SO ₄ [HCl], M	T , K	H^*_{HCl} , M atm ⁻¹
45.0	204.8	1.30e7
	214	3.75e6
	225	1.11e6
45.3	204.7	1.23e7
	202.5	1.38e7
45.0	204.7	1.46e7
	209.8	1.36e7
50.0	222.3	3.23e5
	216.5	5.76e5
	205.1	2.44e6
	199.8	5.00e6

(5). The line shown is a linear regression (forced through zero) for data with $S'_{162}/S'_{146} < 0.04$ (shown as the inset). Data with the largest S'_{162}/S'_{146} (not included in the regression) deviate from the fitted line up to $\sim 20\%$.

The H^*_{HCl} are determined from the solution [HCl] and the partial pressure of HCl, thus these must be known as accurately as possible. The solution [HCl] is known from mixing stoichiometry to a precision of better than 5%, and possible systematic errors (insufficient mixing, evaporation of HCl) are thought to be less than 10%. The CIMS calibration for HCl is estimated to be accurate to $\pm 25\%$. In order for the CIMS signal to reflect the true p_{HCl} in the RWW, full saturation of the He carrier gas passing over the solution is necessary; this was reported for typical flow rates.²⁴ A test was also conducted here for HCl evaporating from 50 wt % H₂SO₄ at 205 K, and the results are shown in Figure 2, a plot of the signal ratio versus the inverse of the total pressure, p_{RWW} ($1/p_{\text{RWW}}$ is proportional to the volume flow rate in the RWW). Excellent linearity is displayed as the volume flow rate was varied over a factor of ~ 8 . Thus significant depletion of solution HCl due to the flow of carrier gas over the liquid does not occur on the time scale of the measurements (tens of minutes for this example). For measurements at lower H^*_{HCl} than for the experiment depicted in Figure 2, low flow rates were used to ensure saturation.

Results and Analysis

The experimental results and certain aspects of the data analysis procedure are presented in this section. Some comparisons with model predictions and previously reported data are also made; more detailed discussions and comparisons are presented in the Discussion section.

HCl Solubility. Listed in Table 1 are the measured H^*_{HCl} for the 45 and 50 wt % solutions at 200–225 K. The uncertainty is estimated to be $\pm 25\%$. The H^*_{HCl} for the 45 and

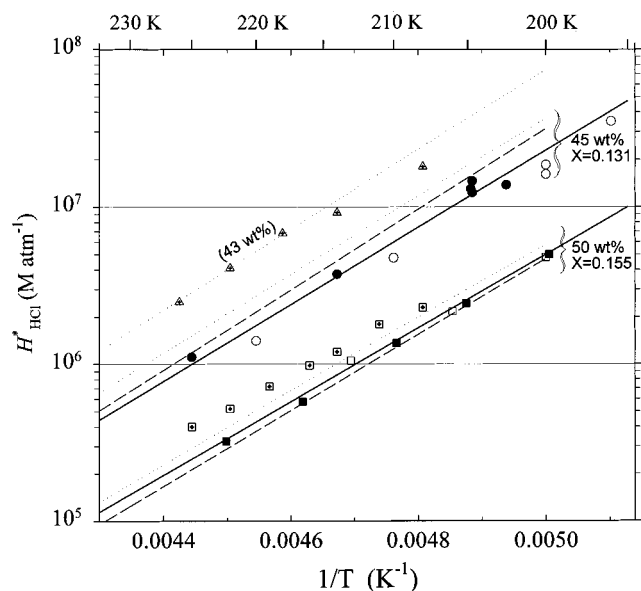


Figure 3. H^*_{HCl} plotted versus inverse temperature for 43, 45, and 50 wt % H₂SO₄ solutions. Filled symbols are data measured here (circles, 45 wt %; squares, 50 wt %), open symbols are data of Hanson and Ravishankara²⁴ reanalyzed here, and symbols with crosses are data of Elrod et al.⁷ (triangles, 43 wt %). The dotted lines are the H^*_{HCl} of Carlsaw et al.,¹⁰ the dashed lines are the Luo et al.²⁹ H^*_{HCl} , and the solid lines are from eq 19.

TABLE 2: H^*_{HCl} from Hanson and Ravishankara^{24,a}

wt % H ₂ SO ₄ [HCl], M	T, K	H^*_{HCl} , M atm ⁻¹
45.0	200	1.85e7
	210	4.76e6
	220	1.41e6
	200	1.61e7
	195	3.50e7
50.0	200	4.80e6
	206	2.17e6
	213	1.05e6
	51.0	205.3
51.0	199	3.48e6
	209.8	8.49e5
	219.5	3.13e5
	199.7	4.01e6

^a These data were reanalyzed as described in the text.

50 wt % H₂SO₄ are also plotted in Figure 3 along with the solubilities of Elrod et al. for 43 and 50 wt % H₂SO₄ and the predicted H^*_{HCl} from the Carlsaw et al.¹⁰ model (dotted lines) and the Luo et al.²⁹ model (dashed lines). The solid lines are the results of least-squares fits to the log H^*_{HCl} vs $1/T$ data and are discussed further below.

Corrections were applied to the previous H^*_{HCl} data from this laboratory.²⁴ The corrected values are listed in Table 2, and some are shown in Figure 3. The previous p_{HCl} was reanalyzed (corrections of 10–25%) in the exact same manner as the data presented here, and the densities of the solutions were taken from Carlsaw et al.¹⁰ (the density of the solutions had been assumed to be negligibly dependent on temperature, the solution [HCl] is increased by ~5%). The corrections to p_{HCl} consisted of the following: (i) The decrease in the SF₆⁻ ion signal during calibrations was mistakenly not taken into account (S'_{146} was 10–20% smaller than S_{146} ; the resulting p_{HCl} are decreased by this amount³⁰), and (ii) during the course of this work it was discovered that the glass tubing downstream of the RWW can be a small source of HCl. In this work, the signal from this “contamination” HCl was typically equal to the “background” count rate in the CIMS (20–50 Hz), thus, in

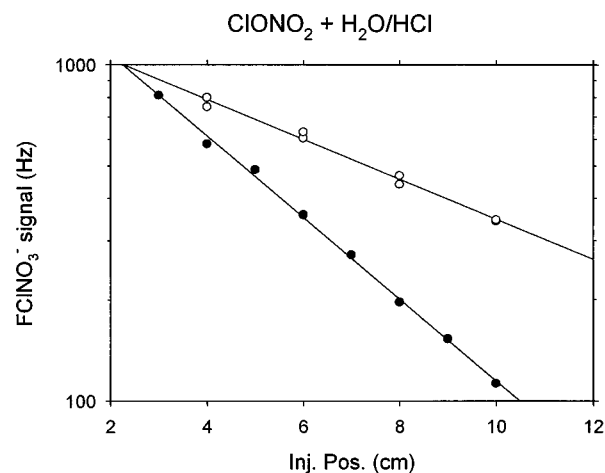


Figure 4. ClONO₂ loss on 49.5 wt % H₂SO₄ at 203 K. Open circles are uptake without added HCl ($p_{\text{HCl}} \leq 4 \times 10^{-12}$ atm), and filled circles are with HCl present ($p_{\text{HCl}} = 1.2 \times 10^{-10}$ atm.) Total pressure was 0.42 Torr (He), and average flow velocity was 1900 cm s⁻¹.

the reanalysis of the previous work, an additional 20–50 Hz was subtracted from the measured signal. Typically, (ii) was a few % or less effect for most of the data; however, it was up to 20% for the 45 wt % data for $T \leq 200$ K.

Reactive Uptake of ClONO₂ on Bulk Liquids. Shown in Figure 4 is the signal due to ClONO₂ (FCINO₃⁻) versus injector position as it was exposed to 49.5 wt % H₂SO₄ at 203 K. Open symbols are data for ClONO₂ + H₂O (residual $p_{\text{HCl}} \leq 4 \times 10^{-12}$ atm), and filled symbols are ClONO₂ uptake in the presence of HCl ($p_{\text{HCl}} = 1.2 \times 10^{-10}$ atm). Reaction probabilities (γ) are calculated from the diffusion corrected first-order loss rates k_{dc} ^{22a} and are also corrected for the non-Maxwellian velocity distribution^{22b} using the equation

$$\frac{1}{\gamma} = \frac{\omega}{k_{\text{dc}}d} + \frac{1}{2}$$

where d is the inner diameter of the flow tube.

Previously, Hanson and Ravishankara² showed that the variation of γ_{R2} with liquid composition (expressed as water activity) could be explained in terms of H , D_1 , and k . They parametrized γ_{R2} and γ_{R1} in terms of water activity for stratospheric conditions. Robinson et al.⁸ examined γ_{R2} (hydrolysis) over a wide range of conditions and presented parametrizations in terms of temperature and H₂SO₄ weight percent, and showed this to be a reasonable description of γ_{R2} . Here, the reaction probabilities measured at 200–205 K are also discussed in terms of solubility, diffusion, and reaction, and these are parametrized using mole fraction of H₂SO₄, X . Mole fraction is a sensible composition variable, and many of the parameters discussed below vary with X in a reasonable way. The conversion between X and wt % H₂SO₄ for H₂SO₄/H₂O solutions is $X = (1 + (100/\text{wt \%} - 1)98.08/18.018)^{-1}$.

ClONO₂ + H₂O. Listed in Table 3 are the reaction probabilities for ClONO₂ + H₂O (γ_{R2}) on sulfuric acid measured in this study (residual $p_{\text{HCl}} < 6 \times 10^{-12}$ atm). The current results for 36–55 wt % H₂SO₄ (203–205 K) are plotted vs wt % H₂SO₄ in Figure 5a along with previously published data.^{2–4,8} In Figure 5b the current results and previous data² from this laboratory (36–65 wt % H₂SO₄ and 200–205 K) are plotted versus mole fraction H₂SO₄, X . Note that the previous γ were corrected for contributions due to R1 (~10% or less). In addition, the γ_0 for 57.5 and 58.5 wt % H₂SO₄ have been revised (0.0064 and 0.0054, respectively) from the earlier work (Table

TABLE 3: Reaction Probability for ClONO₂ + H₂O

wt % H ₂ SO ₄	<i>T</i> , K	γ_{R2}^a
36.5	230	0.086
40.0	230	0.059
45.0	230	0.038
36.5	203	0.113
40.0	203	0.080
45.0	203	0.053
49.5	203	0.028
51.0	203	0.022
53.0	203	0.018
55.0	203	0.011
75	270	1.6×10^{-4}
75	260	1.6×10^{-4}
75	249.5	1.4×10^{-4}
75	240	1.2×10^{-4}
75	230	1.1×10^{-4}
75	217	6.4×10^{-5}
75	208.5	5.0×10^{-5}
75	200	$2.5(\pm 1) \times 10^{-5}$

^a Uncertainty in measurement is $\pm 20\%$ except where noted.

1 in ref 2). In this work residual HCl levels were very low and possible contributions from R1 are negligible.

In the absence of surface reactions, γ_{R2} is described by eq 3 and the chemical terms in γ_{R2} can be separated from the mass accommodation coefficient

$$\Gamma_{R2} = \frac{1}{\frac{1}{\gamma_{R2}} - \frac{1}{\alpha}} \quad (10a)$$

where, from eq 3,

$$\Gamma_{R2} = 4RTH(D_1 k_{R2})^{0.5} / \omega \quad (10b)$$

and k_{R2} is the first-order loss rate coefficient for ClONO₂ hydrolysis in solution. The data in Figure 5b were converted to Γ_{R2} (using $\alpha = 1.0$ in eq 10a) and plotted in Figure 5c versus X . Also shown in Figure 5c is a least-squares fit ($\ln \Gamma_{R2}$ vs X)

$$\Gamma_{R2} = \exp(-0.393 - 13.13X - 50.914X^2) \quad (11a)$$

This expression is used to calculate γ_{R2} as a function of H₂SO₄ content for atmospheric conditions.

The diffusion coefficient for ClONO₂ in sulfuric acid can be estimated from viscosity data;^{31,32} thus the quantity $4RT(D_1)^{0.5}/\omega$ can be calculated, and the quantity $H(k_{R2})^{0.5}$ is obtained using expression (10b). The solid diamonds in Figure 5c are the $H(k_{R2})^{0.5}$ values divided by $1 \times 10^6 \text{ M atm}^{-1} \text{ s}^{1/2}$; the line through these data is a least-squares fit of $\log H(k_{R2})^{0.5}$ vs X . A value for the reacto-diffusive length, l , equal to $(D_1/k_{R2})^{0.5}$, along with D_1 , yields an estimate for k_{R2} . For 60 wt % solutions ($X = 0.216$), l has been measured at 250 K³⁴ and estimated at 203 K² to be $\sim 0.04 \mu\text{m}$, which results in $k_{R2} = \sim 600 \text{ s}^{-1}$ using a $D_1^{31,32}$ of $1 \times 10^{-8} \text{ cm}^2 \text{ s}^{-1}$ at 203 K. This also constrains H to be $\sim 500 \text{ M atm}^{-1}$ for $X = 0.216$ at 203 K.

The variations of H and k_{R2} with X are not known although they are constrained by the values of $H(k_{R2})^{0.5}$. Measurements of the reacto-diffusive length in a range of solutions would help specify the variations of k_{R2} with solution composition. Although these are not presently available, reasonable choices for these variations can be made; two different approaches are presented in this work. In the first approach, ClONO₂ solubility is assumed to have a salt effect dependence on X that is taken to be $1.07(H_{\text{HOCl}})^{0.5}$, where H_{HOCl} is the Henry's law coefficient for HOCl as a function of H₂SO₄ content at 203 K.³³ This H

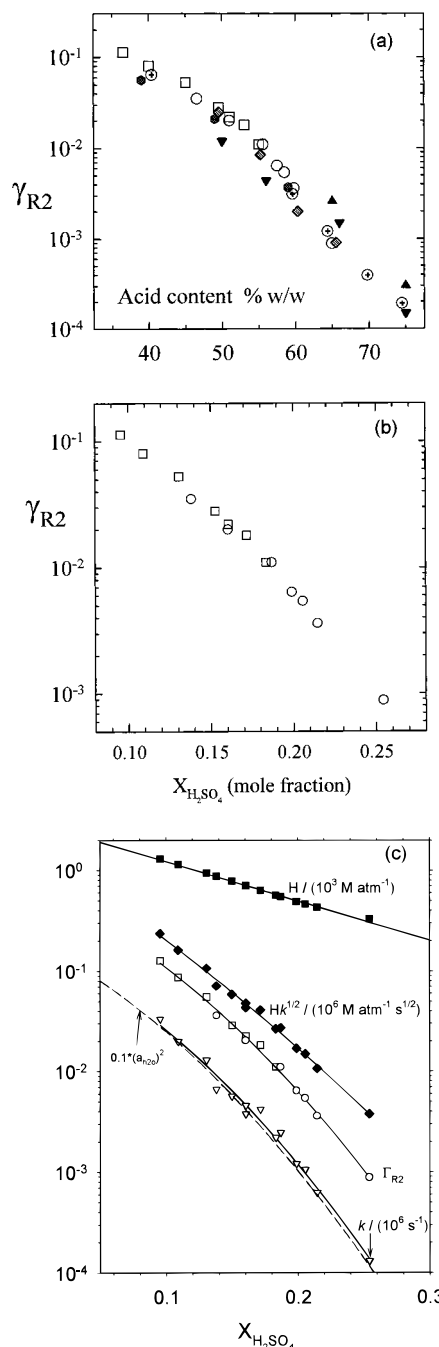


Figure 5. Reaction probability for ClONO₂ + H₂O. (a) γ_{R2} versus H₂SO₄ content: Open squares, this work; open circles, ref 2; circles with cross, ref 4; filled triangles, Tolbert et al.^{3a} and Williams et al.;^{3c} hatched diamonds, Zhang et al.;⁶ hatched hexagons, lowest temperature data from Robinson et al.⁸ (b) Data from this laboratory for temperatures 200–205 K and 65–36 wt % H₂SO₄ plotted versus mole fraction H₂SO₄. (c) $\Gamma_{R2} = 1/(1/\gamma_{R2} - 1)$ from (b) (open circles and squares). The estimated Henry's law coefficient for ClONO₂ (filled squares, eq 11b) are shown divided by 10^3 M atm^{-1} . The quantity $H(k_{R2})^{1/2}$ (filled diamonds, shown divided by $10^6 \text{ M atm}^{-1} \text{ s}^{1/2}$) and the hydrolysis rate coefficient, k_{R2} , are shown (open triangles, divided by 10^6 s^{-1}). The quantity $0.1(a_{\text{H}_2\text{O}})^2$ is shown as the dashed line.¹⁰

is plotted in Figure 5c (solid squares: data divided by 10^3 M atm^{-1}) and a linear regression of $\log H$ vs X is also shown:

$$H = 10^{3.479 - 3.906X} \quad (11b)$$

The dependence for H , H_{HOCl} to the 0.5 power, suggests a smaller salt effect for ClONO₂ than for HOCl.³² The factor

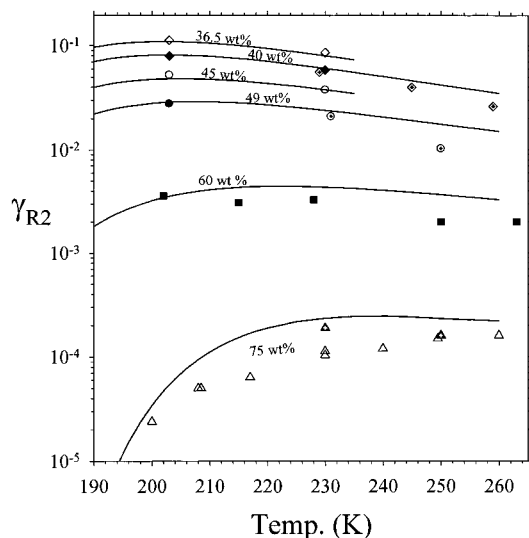


Figure 6. γ_{R2} as a function of temperature. Results from this work: diamonds (open, 36 wt %; filled, 40 wt %); circles (open, 45 wt %; filled, 49.5 wt %) are from Robinson et al.⁸ Filled squares are from previous work in this laboratory.^{2,4,24} Solid lines are the values from Table 3 of Robinson et al.⁸

1.07 was chosen to give a k_{R2} for 60 wt % acid at 203 K of $\sim 600 \text{ s}^{-1}$. Plotted as triangles is the first-order hydrolysis rate k_{R2} (divided by 10^6 s^{-1}) obtained from $H(k_{R2})^{0.5}$ and H . A quadratic least-squares fit of $\log k_{R2}$ vs X results in the equation (shown as the line through the data)

$$k_{R2} = 10^{5.243 - 5.749X - 25.348X^2} \quad (11c)$$

Also shown in the figure as the dotted curve is the square of the activity of water, $a_{\text{H}_2\text{O}}$ (multiplied by 0.1).¹⁰ The close agreement of k_{R2} and this curve suggests that, in this formulation, the hydrolysis rate is proportional to $(a_{\text{H}_2\text{O}})^2$. In a previous description of γ_{R1+R2} , Hanson and Ravishankara² found that k_{R2} was proportional to $(a_{\text{H}_2\text{O}})^{1.8}$. An alternative choice for the dependence of k_{R2} on solution composition, i.e., k_{R2} proportional to water activity, is presented in the Discussion section. Note that the choice of the dependence of k_{R2} on X does not have large atmospheric consequences (see below).

The γ_{R2} for 36, 40, 45, 49, 60, and 75 wt % acid (from Table 3 and previously reported values^{2,4,8,34}) are plotted in Figure 6 versus temperature. For the results on 75 wt % H₂SO₄, there is a marked dependence on temperature over this range, which is qualitatively predicted by Robinson et al.⁸ The lines in Figure 6 are their “predicted” γ_{R2} ; note that this procedure (Table 3 of Robinson et al.⁸) results in γ_{R2} that are substantially different (up to 50%) from the lines shown in their Figure 4.³⁵ Notwithstanding, the predicted values are very close to the measurements reported here for the 36, 40, and 45 wt % H₂SO₄ solutions. For the 75 wt % results, there are discrepancies between the data sets near 230 K and also between the predicted γ_{R2} and the measurements presented here.

From the measurements on 45 wt % at 230 K, the sensitivity of the CIMS for HOCl relative to that for ClONO₂ was determined (assuming stoichiometric conversion of ClONO₂ to HOCl). Then, using this relative sensitivity, the amount of HOCl was found to be equal to the amount of ClONO₂ lost on 75 wt % H₂SO₄. In previous measurements^{2,4} on 75 wt % H₂SO₄ only about 1/2 of the expected HOCl was observed; the implications of this are discussed below.

Reaction of ClONO₂ with HCl. Shown in Figure 7 are the

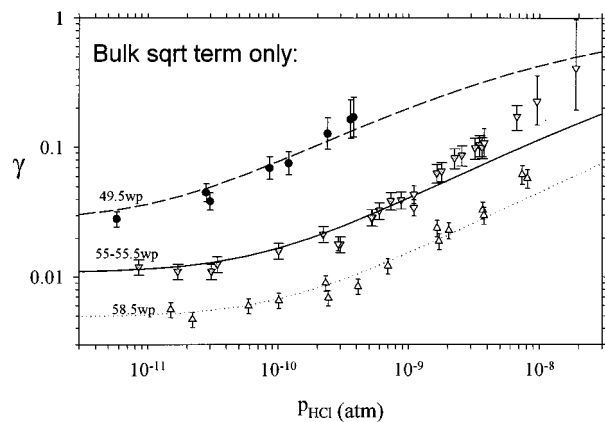


Figure 7. Reaction probability for ClONO₂ plotted as a function of HCl partial pressure for solutions with three different H₂SO₄ contents. The lines are fits to the data according to eq 12, i.e., not including a surface-specific reaction.

reaction probabilities for ClONO₂ on sulfuric acid plotted vs measured p_{HCl} for the 49.5 and 55.0 wt % H₂SO₄ solutions measured in this study and the previous measurements² for the 55.6 and 58.5 wt % solutions (note that the p_{HCl} was reanalyzed for these data² as described above for the previous²⁴ H^*_{HCl} ; in the reanalysis, the previously reported² p_{HCl} was corrected by a maximum of 10 and 25% for the 55.6 and 58.5 wt % measurements, respectively). The current measurements on 55 wt % H₂SO₄ and the previous measurements on 55.6 wt % H₂SO₄ are in excellent agreement. Also shown are dashed lines which are fits to each of the data sets according to the equation

$$\frac{1}{\gamma} = \frac{1}{\alpha} + \frac{\omega}{4RTH\sqrt{D_1}(k_{R2} + k^{\text{II}}H^*_{\text{HCl}}p_{\text{HCl}})} = \frac{1}{\alpha} + \frac{1}{\Gamma_{R2}\sqrt{1 + ap_{\text{HCl}}}} \quad (12)$$

where k^{II} is the second-order rate coefficient for ClONO₂ + HCl/Cl⁻ in solution and $a = k^{\text{II}}H^*_{\text{HCl}}/k_{R2}$. Equation 12 is a modification to eq 3 that takes into account bulk reaction R1 as well as R2. As can be seen in the figure, the fitted lines do not accurately describe the variation of γ with p_{HCl} . A better fit was obtained by Hanson and Ravishankara² by including a term that is linear in HCl and was attributed to a surface reaction between ClONO₂ and HCl.

A recent, improved treatment¹⁶ of surface-specific reactions in liquids resulted in the equation

$$\frac{1}{\gamma} = \frac{1}{S} + \frac{1}{\frac{1}{\Gamma_b} + \frac{1}{\frac{k_{\text{sol}}}{S} + \Gamma_s}} \quad (13)$$

where S is the sticking coefficient,

$$\Gamma_b = 4RTH(D_1k_1)^{1/2}/\omega \quad (13a)$$

is the bulk reaction probability term, where k_1 is the sum of the first-order loss rate coefficients in solution, for this study, $k_{R1} + k_{R2}$,

$$\Gamma_s = 4b'k_s/\omega \quad (13b)$$

is the surface reaction probability term,² where b' is a Langmuir-type equilibrium constant and k_s is the first-order loss rate

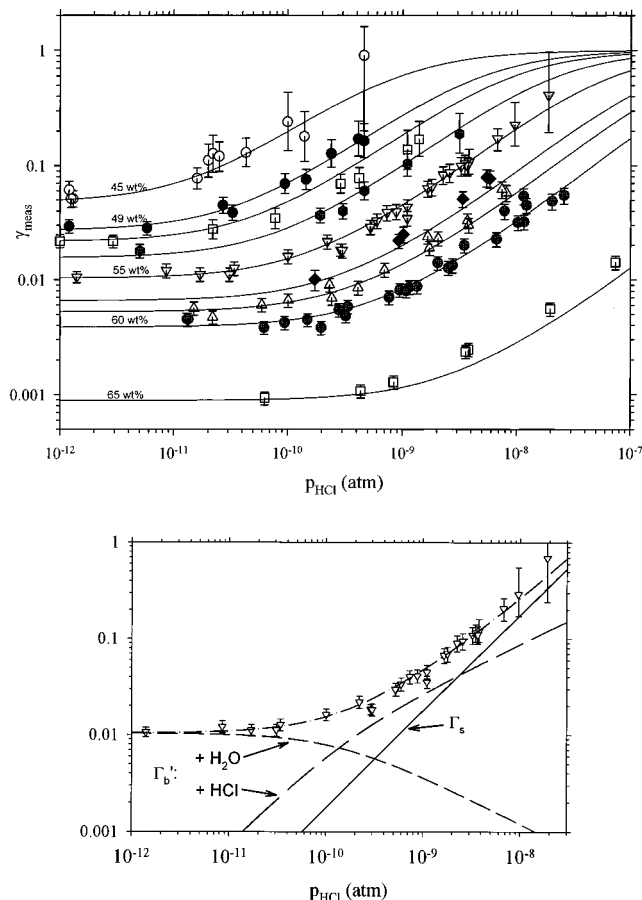


Figure 8. Measured ClONO_2 reaction probabilities for R1 and R2. (a) Top: Data of Figure 6 (49.5, 55, 55.6, 58.5 wt % H_2SO_4) plotted with other data from this work (45, 51, 53) and previous data from this laboratory² (57.5, 59.6–60, and 65 wt % H_2SO_4). The solid lines are the result of a global fit to the data according to eqs 11c and 13–19 (case I). (b) Bottom: Chemical part of the reaction probability, $1/(1/\gamma - 1/S)$, plotted vs p_{HCl} for 55.0 and 55.6 wt % solutions (triangles). Dash-dot line is the predicted γ (eqs 13–18) treated in the same manner and the chemical part is separated into bulk R2 (short-dashed line), bulk R1 (long-dashed line), and surface term (solid line.) See text for details.

coefficient on the surface, and k_{sol} and k_{des} are the rate coefficients for transfer of the molecule from surface to bulk and from surface to gas phase, respectively.¹⁶ Note that Γ_{R2} and Γ_{b} are related: $\Gamma_{\text{b}} = \Gamma_{\text{R2}}(1 + k_{\text{R1}}/k_{\text{R2}})^{1/2}$.

The γ for ClONO_2 on 45–55 wt % H_2SO_4 reported here are plotted in Figure 8a versus p_{HCl} along with the previous measurements² for 55.6–65 wt %. The previous γ for 47 and 51 wt % are of poor quality and were not included; they are in fair agreement with the γ expected from the current results (the scatter of the previous data is large). The curves are a result of a global fit to the data according to eq 13 with S fixed at 1 (see below), $k_{\text{sol}}/k_{\text{des}}$ fixed at 10, and

$$\Gamma_{\text{b}} = \Gamma_{\text{R2}} \sqrt{1 + a_0 D_{\text{rel}} \frac{H^*_{\text{HCl}} p_{\text{HCl}}}{k_{\text{R2}}}} \quad (14)$$

where Γ_{R2} are from Table 3 (Γ_{R2} from eq 11a is within 10% of these values), $a_0 D_{\text{rel}}$ is equal to the second-order rate coefficient k^{II} for $\text{ClONO}_2 + \text{HCl}$, and k_{R2} as a function of X is given by eq 11c. a_0 is a fitted parameter, D_{rel} is a function of X , and is D_1 relative to the value for 60 wt % acid³² (see eq 16). This form for k^{II} contains the assumption that it varies with the

TABLE 4: Parameters for Global Fit

wt % H_2SO_4	X	T , K	Γ_{R2}	H^*_{HCl} , $^{\circ}\text{M atm}^{-1}$
45	0.131	202.5	0.0555	1.59e7
45	0.131	204.6	0.0555	1.20e7
49.5	0.153	202.8	0.0288	3.90e6
51	0.161	203	0.0225	2.30e6
53	0.172	203	0.0183	1.11e6
55	0.183	203	0.0111	5.20e5
55.6	0.187	203	0.0111	3.80e5
57.5	0.199	203	0.00644	1.77e5
58.5	0.206	203	0.00543	1.16e5
59.8	0.215	203	0.00361	7.00e4
65	0.254	203	0.000881	7.40e3

^a From eq 19.

diffusion coefficient, i.e., that R1 is likely a diffusion-limited reaction. The H^*_{HCl} were obtained by a fit to the data (see eq 19 below).

The surface-specific reaction probability for $\text{ClONO}_2 + \text{HCl}$ is parametrized as

$$\Gamma_{\text{s}} = b_0 B_{\text{rel}} H^*_{\text{HCl}} p_{\text{HCl}} \quad (15)$$

where b_0 is a fitted parameter and B_{rel} is a function of X to take into account the variations of the adsorption equilibrium constant and second-order surface rate coefficient with X . The global fit discussed here (referred to as case I) contains the assumption that B_{rel} is proportional to the activity of water, $a_{\text{H}_2\text{O}}$. This is the variation used by Hanson and Ravishankara² for the surface reaction term. Another assumption in this treatment (eq 15) is that the ratio of the surface coverage of HCl to the $[\text{HCl}]$ in the bulk is independent of X .

The diffusion coefficient for HOCl of Huthwelker et al.³² is used as a proxy for the D_1 for ClONO_2 , and a fit of this at 203 K results in

$$D_1(X) = 10^{-7.815 + 5.679X - 29.252X^2} \quad (16a)$$

$$D_{\text{rel}}(X) = 10^8 D_1(X) \quad (16b)$$

The activity of water, $a_{\text{H}_2\text{O}}$, at 203 K was calculated using the Carslaw et al.¹⁰ model for a range of H_2SO_4 contents and a least-squares fit to $a_{\text{H}_2\text{O}}$ vs X resulted in

$$a_{\text{H}_2\text{O}} = 10^{0.151 - 3.338X - 11.896X^2} \quad (17a)$$

$$B_{\text{rel}}(X) = a_{\text{H}_2\text{O}}(X) \quad (17b)$$

Table 4 is a list of the experimental conditions, and the Γ_{R2} and H^*_{HCl} used in the fits for each set of measurements. The parameters a_0 and b_0 were obtained using a nonlinear weighted least-squares fitting routine, and the values

$$a_0 = 1.69 \times 10^7 \text{ M}^{-1} \text{ s}^{-1} \quad b_0 = 257 \text{ M}^{-1} \quad (18)$$

were obtained. The standard deviations of the parameters are $\sigma_{a_0} = 2.8 \times 10^6 \text{ M}^{-1} \text{ s}^{-1}$ and $\sigma_{b_0} = 34 \text{ M}^{-1}$. Using k_{R2} from eq 11c and $B_{\text{rel}} = a_{\text{H}_2\text{O}}$ (eq 17b) and the fitted values (eq 18) is case I. Alternative fits to the data in Figure 8a (cases II and III) using different formulations for k_{R2} and Γ_{s} are presented below.

The contributions of the bulk and surface terms to the reaction probability are shown in Figure 8b for the 55.0 and 55.6 wt % solutions. The measured (triangles) and fitted (dash-dot line) reaction probabilities are plotted as $1/(1/\gamma - 1/S)$ vs p_{HCl} . Treating the data in this manner separates S from the chemical

TABLE 5: Reaction Probabilities, Vapor Pressures, and HCl Solubility Measurements for H₂O/H₂SO₄/HNO₃ Solutions with Solution Composition Given in wt % HNO₃/wt % H₂SO₄ and (HNO₃ Molal/H₂SO₄ Molal) and All Measurements at 205 K Except Where Noted

obs p_{HNO_3} , 10 ⁻⁹ atm	pred ^c p_{HNO_3} , 10 ⁻⁹ atm	obs p_{HCl} , 10 ⁻¹⁰ atm	[HCl] {wf × 10 ⁻⁵ }, ^d 10 ⁻³ M	γ	H^*_{HCl} , M atm ⁻¹	H^*_{HCl} (ref 10)	H^*_{HCl} (ref 29)	froz ^e p_{HNO_3} , 10 ⁻⁹ atm	froz γ
Solution A: 4.4/44.6 (1.3 m/8.89 m)									
2.7	2.2	≤0.1	0	0.019		6.6e6	4.1e6		
2.8	2.2	2.3	{1.8} 0.74	0.084	3.2e6				
2.6	2.2	3.6	{3.6} 1.4	0.12	4.0e6				
2.5	2.2	7.3	{6.6} 2.6	0.20	3.6e6				
Solution B: 7.9/39.6 (2.4 m/7.7 m)									
1.8 ^a	2.3	≤0.1	0	0.021		1.5e7	8.5e6		
2.0 ^a	2.3	1.4	{2.6} 1.0	0.085	7.1e6				
2.0 ^a	2.3	4.0	{8.2} 3.1	0.20	7.8e6				
2.1	2.7	≤0.1	0	0.024		1.4e7	7.4e6		
3.5	2.7	1.7	{2.7} 1.1	0.088	6.4e6				
3.2	2.7	2.8	{4.8} 1.9	0.084	6.7e6				
3.8	2.7	0.76	{1.5} 0.57	0.045	7.4e6				
Solution C: 16.8/30.0 (5.0 m/5.8 m)									
3.8 ^b	3.2	≤0.25	0	0.027		3.3e7	1.3e7		
2.7 ^{b,f}	3.2	0.63 ^f	{2.0} 0.75	0.083 ^f	1.2e7			0.67 ^g	0.16
3.7 ^b	3.2	1.2	{5.5} 2.0	0.15	1.7e7				
2.1 ^{b,f}	3.2	≤0.1	0	0.026 ^f				0.67 ^g	0.044
2.3 ^b	3.2	0.5	{1.9} 0.69	0.084	1.4e7				
2.5 ^b	3.2	1.4	{4.8} 1.8	0.10	1.3e7				
Solution D: 25.6/20.3 (7.5 m/3.8 m)									
~4 ^f	3.2	≤0.13	0	0.058 ^f		6.7e7	2.4e7	0.44 ^h	0.093
2.7	3.2	0.45	{3.8} 1.3	0.065	2.8e7			0.38 ^h	0.16
3.5	3.2	1.0	{8.7} 3.0	0.10	3.0e7			0.46 ^h	0.19

^a 204 K. ^b 204.5 K. ^c Predicted p_{HNO_3} from Carslaw et al.¹⁰ ^d Weight fraction of HCl is given in braces. [HCl] in molar was calculated using $\rho = 1.44, 1.40, 1.35,$ and 1.30 g cm^{-3} for solutions A–D, respectively. ^e Measurements taken over mixed phase (solid/liquid) solutions. The A or B solutions did not freeze. ^f These data were taken over a solution that had begun to freeze (i.e., solid phase was growing). ^g The p_{HNO_3} over NAT for these conditions is $4.8 \times 10^{-10} \text{ atm}$.³⁹ ^h The $p_{\text{H}_2\text{O}}$ increased by 22% (on average) after the D solutions had froze. The p_{HNO_3} over NAT for these conditions is $2.1 \times 10^{-10} \text{ atm}$.³⁹

terms and also allows for partitioning of the bulk and surface terms. This quantity is equal to the quantity $\Gamma_b' + \Gamma_s$ from eq 13 where $\Gamma_b' = (1/\Gamma_b + k_{\text{des}}/(S k_{\text{sol}}))^{-1}$. The bulk part of R1 is equal to $\Gamma_b' k_{\text{R1}}/(k_{\text{R1}} + k_{\text{R2}})$ (long dash), the surface part is Γ_s (solid line), and $\Gamma_{\text{R2}} = \Gamma_b' k_{\text{R2}}/(k_{\text{R1}} + k_{\text{R2}})$ (short dash). Γ_b and Γ_s are taken from the fitted parameters (eqs 14–18), S is taken to be 1, and $k_{\text{sol}}/k_{\text{des}}$ is fixed at 10. In the log–log plot shown in Figure 8b, the surface term has a slope of 1, and the bulk R1 term has a slope of 1/2 at high [HCl] when R2 is negligible. At 203 K, this model (case I) predicts that the surface term is dominant for p_{HCl} above $2.5 \times 10^{-9} \text{ atm}$ ([HCl] = 10^{-3} M). For the solutions studied here, the fit suggests that when bulk [HCl] is greater than $\sim 10^{-3} \text{ M}$, the surface term for R1 becomes dominant.

HNO₃/H₂SO₄/H₂O Solutions. Solutions composed of 44.6/4.4 (wt % H₂SO₄/wt % HNO₃), 39.6/7.9, 30.0/16.8, and 20.3/25.6 were prepared and doped with varying amounts of HCl (these solutions are referred to as solutions A–D, respectively). These compositions correspond to those expected for liquid supercooled solutions exhibiting vapor pressures of H₂O of $2.64 \times 10^{-7} \text{ atm}$ and of HNO₃ of $\sim 2.4 \times 10^{-10} \text{ atm}$ at 193.0 (A), 192.2 (B), 191.5 (C), and 190.9 K (D).¹⁰ These partial pressures correspond to $\sim 5 \text{ ppmv H}_2\text{O}$ and $\sim 5 \text{ ppbv HNO}_3$ in the lower stratosphere ($\sim 19 \text{ km}$ altitude). γ_{R1} and γ_{R2} were measured on these solutions at $\sim 205 \text{ K}$ (where $p_{\text{H}_2\text{O}}$ and p_{HNO_3} are about 2×10^{-6} and $1.5 \times 10^{-9} \text{ atm}$, respectively). These solutions were also doped with varying amounts of HCl, and [HCl] was determined from the mixing stoichiometry.

Samples of the solutions were titrated with a standardized NaOH solution before and after the experiments were performed. The amount of [H⁺] in the starting solutions was 0.1–0.5% greater than that expected from the mixing stoichiometry while [H⁺] in samples after experiments were performed was generally

$\sim 1\%$ greater than expected. This is equivalent to $\sim 0.5 \text{ wt } \%$ in H₂SO₄. This could be due to a loss of water vapor from the solutions during the experiments; i.e., the $p_{\text{H}_2\text{O}}$ in the carrier gas, which was set according to the predictions of Carslaw et al.,¹⁰ was a little lower than the partial pressure of H₂O exhibited by the solutions.

For solution D (and on occasion for C), crystalline solids nucleated in a few spots in the solution after tens of minutes and grew slowly, extending throughout the solutions in about 1 h. The solutions did not freeze completely; there was liquid present after the crystals had grown throughout the solutions. The reaction probability for ClONO₂ was also investigated over these mixed-phase solutions.

Listed in Table 5 are the compositions of the solutions investigated, the measured ClONO₂ reaction probabilities, the observed p_{HNO_3} and p_{HCl} (also p_{HNO_3} over the mixed-phase solutions), the measured H^*_{HCl} , and the H^*_{HCl} 's from the Luo et al.²⁹ and Carslaw et al.¹⁰ models. The reaction probabilities are plotted in Figure 9 versus [HCl] along with the predicted values for pure sulfuric acid (solid lines). The predicted values were obtained from case I, eqs 13–18 with $H^*_{\text{HCl}}/p_{\text{HCl}}$ replaced by [HCl]. The $\gamma_{\text{R1}+\text{R2}}$ for solutions B–D are significantly lower than that predicted for the corresponding pure sulfuric acid solutions: approximately a factor of 2 lower with the discrepancy increasing with the amount of HNO₃ in solution. The dashed lines are modifications to case I and are discussed below.

The vapor pressures of HNO₃ over the solid/liquid mixtures that formed in solutions C and D are consistent with nitric acid trihydrate (NAT); the p_{HNO_3} is within a factor of 2 of that predicted for NAT.³⁹ The vapor pressure of H₂O over solution D was also monitored before and after solids formed and was found to increase $\sim 20\%$ upon freezing. From the measured p_{HNO_3} and the calculated $p_{\text{H}_2\text{O}}$ (taking into account the relative

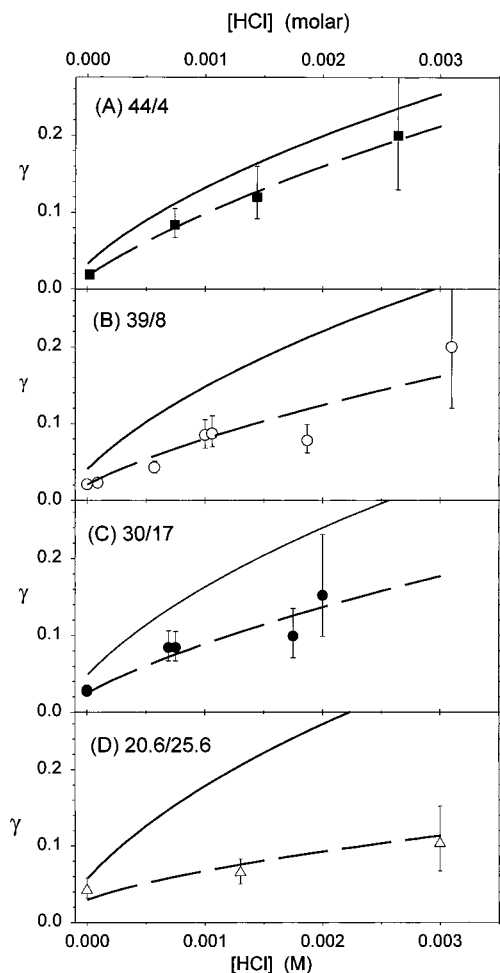


Figure 9. Reaction probability for ClONO_2 plotted as a function of $[\text{HCl}]$ for solutions containing HNO_3 . The solid lines are the predictions (case I, eqs 13–18) for the binary H_2SO_4 solutions exhibiting the same $p_{\text{H}_2\text{O}}$. The H_2SO_4 contents for $p_{\text{H}_2\text{O}} = 2.64 \times 10^{-7}$ atm and $T = 193, 192.2, 191.5,$ and 190.9 are 48.2, 46.6, 45.0, and 43.5 wt %. The approximate wt % H_2SO_4 /wt % HNO_3 is indicated in the figure. Data for solution A, 1.3 m HNO_3 and 8.9 m H_2SO_4 . Solution B contains 2.4/7.7, solution C contains 5.0/5.8, and solution D contains 7.5/3.8 m HNO_3 /m H_2SO_4 . The dashed lines are modified case I predictions: Γ_b is divided by 2 in each case; Γ_s is unchanged for (A), divided by 2 for (B) and (C), and divided by 10 for (D).

change in $p_{\text{H}_2\text{O}}$ for solution D and assuming no change for (C), the Carslaw et al.¹⁰ model gives that the liquid solution remaining after C had frozen contained 43 wt % (8.0 m) H_2SO_4 and 2.4 wt % (0.7 m) HNO_3 and that for D contained 36.3 wt % H_2SO_4 (6.3 m) and 4.5 wt % HNO_3 (1.2 m). Assuming that H_2SO_4 was not incorporated into the solid, the differences in the compositions of the remaining liquid and the starting solution imply that a solid with H_2O to HNO_3 ratios of 3.4 and 3.2 for solutions C and D, respectively, had formed. Considering the experimental and computational uncertainties, these ratios are consistent with the formation of the NAT solid in these solutions.

γ for ClONO_2 on Particles. The uptake of ClONO_2 onto small sulfuric acid particles (49 ± 1 wt % H_2SO_4 doped with HCl) was studied at 240 K to investigate S and α . When $\gamma \rightarrow 1$, these measurements are much less sensitive to gas-phase diffusion than bulk measurements, resulting in a more accurately measured γ and thus a better limit to S . Measurements of ClONO_2 loss were performed for two HCl levels: $p_{\text{HCl}} = 1.1$ and 2.0×10^{-7} atm. The particles had a surface area weighted mean radius, r_s ,¹⁷ of $0.08 \mu\text{m}$, and the number density was $(2-5) \times 10^5 \text{ cm}^{-3}$.

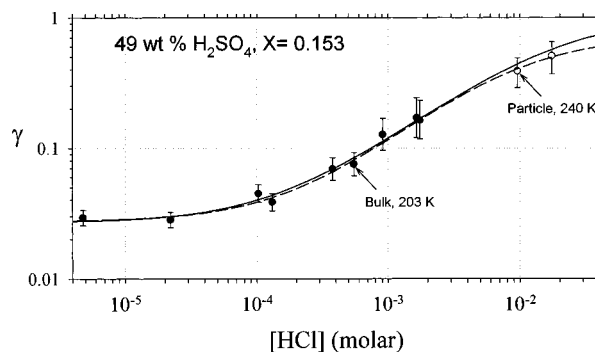


Figure 10. Reaction probability for ClONO_2 plotted as a function of HCl content for 49.5 ± 0.5 wt % H_2SO_4 at 203 K (filled circles) and 49 ± 1 wt % H_2SO_4 particles at 240 K (open circles). The solid line is the predicted γ according to eqs 11c, and 13–18, and the dashed line is a fit of the data according to eqs 13–15.

The $\gamma_{\text{R1+R2}}$ were measured to be $0.38(\pm 0.1)$ and $0.51(\pm 0.14)$, for $p_{\text{HCl}} = 1.1$ and 2.0×10^{-7} atm, respectively. A few measurements were averaged, and the uncertainties are twice the standard error of the mean. H^*_{HCl} is $8.7 \times 10^4 \text{ M atm}^{-1}$ for these conditions,¹⁰ and the HCl content of the particles was 9.6×10^{-3} and 1.7×10^{-2} M, respectively. These γ provide a lower limit to S , the sticking coefficient for ClONO_2 (or possibly also the mass accommodation coefficient¹⁶). Because γ is still increasing with HCl in these experiments, it is likely that Γ_b and/or Γ_s are not large enough to force the measured γ to the value of S (see eq 13), and thus S is likely to be greater than 0.5.

This can be taken into account in a crude manner. The measured reaction probabilities on 49 ± 1 wt % aerosol particles at 240 K (open circles) and the reaction probabilities measured on 49.5 ± 0.5 wt % acid at 203 K (filled circles) are plotted vs HCl content in Figure 10. The dashed line is a fit of these data using eqs 13–16, replacing $H^*_{\text{HCl}}p_{\text{HCl}}$ with $[\text{HCl}]$ and letting a_0 , b_0 , and S vary. The solid line is the predicted γ for eqs 13–18 (case I), with S set equal to 1 ($k_{\text{sol}}/k_{\text{des}} = 10$ for both cases). Note that the reacto-diffusive depth, l , for these conditions is much smaller than the particle radius r_s ; thus, the size dependent term,¹⁶ $\coth(r_s/l) - l/r_s$, is equal to 1. The data appear to be well-described by either approach, and thus γ (for a given $[\text{H}_2\text{O}]$ or $[\text{HCl}]$) is not strongly dependent on temperature over this range, which has been pointed out previously.^{2,7} For the dashed line, the fit yielded a value of $S = 0.72(\pm 0.1; 95\% \text{ confidence level})$. The value of S from this fit is probably more uncertain than the 95% confidence level indicates because the assumption that a_0 and b_0 do not depend on temperature is critical to extracting accurate information about S using this approach. The agreement with the predicted γ (solid line, eqs 13–18) show that a value of unity for S is consistent with the measurements and that a_0 and b_0 are probably not strongly temperature dependent. The temperature dependence of the reaction probabilities is discussed further below.

Discussion

H^*_{HCl} . The reanalyzed²⁴ and new 50 wt % H^*_{HCl} data from this laboratory are in excellent agreement and also agree well with the Luo et al.²⁹ values (within 10%) and the H^*_{HCl} of Carslaw et al.¹⁰ (within $\sim 20\%$). For the 45 wt % solutions, the agreement is not as good: the reanalyzed 45 wt % H^*_{HCl} data are about 25% lower than the results presented here which in turn lie about 20 and 35% below the predicted H^*_{HCl} of Luo et al. and Carslaw et al., respectively. The reason for the

difference between the current measurements and previous²⁴ H^*_{HCl} for 45 wt % is not known; it is about equal to the uncertainty in the measurements. For example, because the solutions are not known exactly (titrated to an accuracy of ± 0.5 wt %), it is possible that the solutions in the earlier work were slightly more concentrated (a 0.5 wt % change results in a variation in H^*_{HCl} of $\sim 20\%$). Note that discrepancies of $\sim 30\%$ should not be considered serious. This level of agreement between measurements and models is satisfactory at this stage of model development and experimental technique.

However, some experimental results are not in agreement with the consensus. The 50 wt % results of Zhang et al.³⁶ are about $1/4$ of those shown in Figure 3; as discussed by Elrod et al.,⁷ their measurements³⁶ probably suffered from instrument calibration errors. The Tabazadeh et al. model,³⁷ which was fit to the H^*_{HCl} values reported by Zhang et al., not surprisingly gives 50 wt % values that are also about $1/4$ of the solid or dashed lines. HCl solubilities for 50 wt % H₂SO₄ determined from time-dependent uptake measurements, where a value for $H^*_{\text{HCl}}D_1^{0.5}$ is obtained,^{24,31a} are in reasonable agreement with those shown in Figure 3: the H^*_{HCl} of Williams and Golden^{31a} are in good agreement while the values of Hanson and Ravishankara²⁴ (using the same D_1 for HCl) are about $1/3$ of the solid line. In general, solubilities determined from time-dependent uptake measurements are not as accurate as that detailed above.³⁸

The present and previous data (Tables 1 and 2) for 45 and 50 wt % H₂SO₄, the data of Elrod et al.⁷ for 43 and 50 wt % H₂SO₄, and H^*_{HCl} from the Carslaw et al.¹⁰ model for 55, 60, and 65 wt % H₂SO₄ (at 190–220 K in 5 K intervals) were fit to the equation

$$H^*_{\text{HCl}} = \exp(c_0 + (d_0 + d_1X)/T)(e_0 + e_1X + e_2X^2) \quad (19a)$$

where X is mole fraction of H₂SO₄. The values from the Carslaw et al. model¹⁰ were used because reliable experimental data in solutions ≥ 55 wt % are lacking (note that at 250 K in 60 wt % H₂SO₄ this model agrees very well with a measured H^*_{HCl} ¹⁸). Equation 19a is similar to the equation presented by Hanson and Ravishankara² parametrized in terms of mole fraction rather than water activity. Values of the parameters from the fit are

$$c_0 = -9.021 \quad e_0 = 0.363 \quad e_1 = -2.616 \quad e_2 = 4.995 \quad (19b)$$

where the values $d_0 = 6922$ and $d_1 = -9800$ were fixed and obtained from a fit of $\ln H^*_{\text{HCl}}$ as a function of X : $\ln H^*_{\text{HCl}} = C_X + (d_0 + d_1X)/T$ (H^*_{HCl} as a function of T was obtained from Luo et al.²⁹ for 55–65 wt % and to the data reported here for 45 and 50 wt % H₂SO₄).

ClONO₂ + H₂O. The reaction probability for ClONO₂ hydrolysis can be explained in terms of solubility, diffusivity, and reactivity as given in eq 3. The variation of these parameters with H₂SO₄ content and with temperature (see below) is reasonable. This is in general agreement with the conclusions of Hanson and Ravishankara² and Robinson et al.⁸

As depicted in Figure 6, the temperature dependence of γ_{R2} for the 36, 40, and 45 wt % solutions measured here is similar to that presented by Robinson et al.⁸ (these γ_{R2} , as well as for 60 wt %, ^{2,4} have effective activation enthalpies of approximately -1 kcal mol⁻¹). This weak T -dependence is due to a cancellation of terms, as discussed previously by Hanson and Ravishankara.² Also evident in the figure is that the T -dependence of the measured γ_{R2} for 75 wt % acid is much

different than that predicted by Robinson et al.,⁸ which is probably due to their estimation procedure for D_1 .

Their calculated D_1 led to other conclusions that may be erroneous. For example, the slight downturn in γ_{R2} for 36–49 wt % H₂SO₄ as temperature is decreased to 190 K can be traced to the temperature dependence of D_1 . These D_1 are extrapolated outside the temperature range of the measured viscosities, upon which the D_1 are based, and thus have considerable uncertainty.⁴² Their postulate that an acid-catalyzed hydrolysis channel must be included to explain γ_{R2} in strong acids (> 65 wt % H₂SO₄) is also influenced by their D_1 : the D_1 in 75 wt % H₂SO₄ at 203 K of other researchers^{31,32} is $\sim 3 \times 10^{-10}$ cm² s⁻¹ while the Robinson et al.^{8,35} value is 3×10^{-12} cm² s⁻¹.

The postulate of an acid-catalyzed mechanism for R2 in strong acid also depends on the choice of H and k_{R2} . They modeled H on the solubility of HOCl, H_{HOCl} , as done here for case I; however, they used H_{HOCl} ³² that have since been shown³³ to be erroneous in strong H₂SO₄ solutions. Here the H_{HOCl} of Donaldson et al.³³ was used to obtain eq 11b. It should be noted that assumptions about H strongly influence the interpretation of the measured γ_{R2} ; indeed H_{HOCl} may not be a good model for H in strong acids. The γ_{R2} measured here for 75 wt % H₂SO₄ ($X = 0.355$), $\sim 3(\pm 1.5) \times 10^{-5}$ (interpolated to 203 K), with that obtained by extrapolating eq 11a, $\gamma_{\text{R2}} = 1.1 \times 10^{-5}$, shows fair agreement. There does not seem to be evidence that a different mechanism for the hydrolysis of ClONO₂ operates in strong acids.

For the 75 wt % H₂SO₄ results at 230 K, there is a difference in the previous γ_{R2} ^{3c,4} and those reported here. A possible explanation for a positive deviation of a measurement from the true γ_{R2} is the presence of a reactive contaminant in the solution. In the previous measurements on 75 wt % H₂SO₄ from this laboratory, the HOCl produced was not equal to the amount of ClONO₂ lost,⁴ prompting Hanson and Ravishankara² to suggest that ClONO₂ reacted with a component of the solution other than H₂O. It is possible that the solutions in the previous measurements had small amounts of dissolved impurities that could react with ClONO₂, such as organic compounds⁴³ (also noted for HOCl³³). Note that the γ_{R2} for 75 wt % H₂SO₄ would be affected by impurities more than less acidic solutions because [H₂O] and thus the rate for R2 is the lowest.

ClONO₂ + HCl. The solubility of HCl is an important parameter in determining γ for ClONO₂. Therefore, the choice of which H^*_{HCl} to use in a fitting or extrapolation procedure is important, especially in the more dilute H₂SO₄ solutions (i.e., 55 wt % H₂SO₄ and lower). If inaccurate H^*_{HCl} are used, interpretation of the values of a_0 and b_0 in terms of ClONO₂ solubility or adsorption (H or b'), diffusivity (D_1), or reactivity ($k^{\text{HCl/H}_2\text{O}}$ or k_s) would be flawed. Note that extrapolation of the reaction probability outside of the range of measured temperatures will be true to the data as long as H^*_{HCl} does not vary with temperature unexpectedly and that the constants a_0 and b_0 do not vary significantly with temperature.

It is assumed that Γ_{R2} , a_0 , and b_0 do not depend strongly on temperature. As discussed above, this is a good assumption for Γ_{R2} . Also, the reaction probability for R1 was constant as the temperature was varied from 198 to 208 K for a 47 wt % H₂SO₄ solution containing 10^{-3} M HCl² (similar results were also reported by Elrod et al.⁷). This was attributed to a cancellation of terms,² where, for example, solubility H has a temperature dependence corresponding to ~ -10 kcal mol⁻¹ solvation enthalpy, and diffusivity D_1 and reaction k_{R2} are both activated by ~ 10 kcal mol⁻¹ (recall that γ depends on $H(D_1k)^{0.5}$, eq 3). In addition, the constant a_0 , equal to the second-order

TABLE 6: Comparison to Published Data for γ_{R1+R2} on Sulfuric Acid and $\text{HNO}_3/\text{H}_2\text{SO}_4/\text{H}_2\text{O}$ Solutions

<i>T</i>	H_2SO_4 wt %	HNO_3 wt %	density, g cm^{-3}	[HCl], 10^{-3} M	γ^a (ref 6)	γ (ref 7)	γ^b (this work)
203	55	0	1.52	0.12		0.010	0.022 ± 0.005
203	51	0	1.47	0.97		0.038	0.08 ± 0.02
203	49	0	1.45	2.3		0.061	$0.18 \pm^{0.1}_{0.05}$
203	45	0	1.41	13		0.12	$0.5 \pm^{0.5}_{0.25}$
197	49	0		5.8	0.16 ± 0.06		$0.24 \pm^{0.12}_{0.06}$
198.5	51	0		2.2	0.10 ± 0.05		$0.13 \pm^{0.04}_{0.03}$
201	55	0		0.33	0.04 ± 0.01		0.032 ± 0.006
205.5	60	0		0.025	0.009 ± 0.002		0.0057 ± 0.001
205	44.4	4.4	1.44	2.4			$0.18 \pm^{0.1}_{0.05^c}$
203	44	6.1	1.4	2.4		0.048 ^c	
205	39.6	7.9	1.4	2.4			$0.16 \pm^{0.1}_{0.05^c,d}$
203	36.2	12.6	1.34	6.8		0.07 ^d	
205	30	17	1.34	6.8			$0.18 \pm^{0.1}_{0.05^d}$
203	20.2	28.3	1.25	17		0.11 ^e	
205	20.3	25.6	1.3	17 ^e			$0.25 \pm^{0.15}_{0.07^e}$

^a The errors for Zhang et al.⁶ were assigned by estimating the scatter in the measurements. ^b “This work” reaction probabilities are interpolated. HCl-content determination is detailed in the text. Uncertainties are that for a typical measurement (nonsymmetric errors are obtained when $\gamma > 0.1$). ^c These points should be compared; this work (interpolated according to the [HCl] calculated) versus Elrod et al. ^d These points should be compared as in c. ^e These points should be compared; value from “this work” involves a large extrapolation.

rate coefficient for $\text{ClONO}_2 + \text{HCl}$ in 60 wt % H_2SO_4 at 203 K, was shown to have essentially the same temperature dependence as k_{R2} between 250 and 202 K in 60 wt % H_2SO_4 .^{2,34}

As discussed above, the bulk results (203 K) and the particle results (240 K) on ~ 49 wt % acid can be described using temperature-independent values for the parameters a_0 and b_0 . The particle measurements are in the regime where the surface term (b_0) is dominant; thus it is likely that b_0 is not strongly temperature dependent, at least for ~ 49 wt % H_2SO_4 .⁴¹ The constant b_0 is proportional to the quantity $b'k_s^{\text{II}}/T^{1/2}$, where k_s^{II} ($=k_s/[\text{HCl}]_s$) is the second-order rate coefficient between adsorbed HCl and ClONO_2 . Thus, for b_0 to be not strongly dependent on temperature, the temperature dependency of b' must be nearly matched by compensating variations in k_s^{II} with temperature. Additional measurements of the surface reaction term over a range of temperatures are needed to further specify its temperature dependency.

Comparison of γ for $\text{ClONO}_2 + \text{HCl}$ with Previous Measurements. The current measurements of γ_{R1} and γ_{R2} are in good agreement with the previous measurements from this laboratory,² and both sets of data were used in the fitting procedure. The parameter a_0 corresponds to the quantity ρ in Hanson and Ravishankara,² and these are in good agreement. The last term in eq 14, $a_0 D_{\text{rel}}[\text{HCl}]/k_{R2}$, is equal to the quantity $\rho[\text{HCl}]/a_{\text{H}_2\text{O}}$ from ref 2. Thus

$$\rho = a_0 D_{\text{rel}} a_{\text{H}_2\text{O}} / k_{R2} \quad (20)$$

For 60 wt % H_2SO_4 ($X = 0.216$), $a_0 D_{\text{rel}} = 1.7 \times 10^7 \text{ M}^{-1} \text{ s}^{-1}$, $k_{R2} = 600 \text{ s}^{-1}$, and $a_{\text{H}_2\text{O}} = 0.075$ and (20) results in a value for ρ of 2100 M^{-1} , very close to the value $\rho = 2000 \text{ M}^{-1}$ found previously.^{2,44} The a_0 of (18) results in a value for the second-order rate coefficient for R1 of $1.7 \times 10^7 \text{ M}^{-1} \text{ s}^{-1}$ for 60 wt % H_2SO_4 at 203 K. This is comparable to the diffusion limited² rate coefficient of $\sim 8 \times 10^6 \text{ M}^{-1} \text{ s}^{-1}$ using a value for D_1 of $1 \times 10^{-8} \text{ cm}^2 \text{ s}^{-1}$ and a capture radius of 10 \AA .

The parameter b_0 for Γ_s in the current formulation (case I, eqs 16–18) is less than the equivalent parameter k''_{sur} for Γ_s in the previous formulation.² Thus the case I fit indicates the reaction on the surface contributes less to γ_{R1} than the previous fit implied.

The reaction probabilities for ClONO_2 (R1 + R2) on $\text{H}_2\text{SO}_4/\text{H}_2\text{O}$ of Elrod et al.⁷ and Zhang et al.⁶ are compared to this work in Table 6. Elrod et al.⁷ report HCl content in weight fraction which was converted to molarity using the H_2SO_4

solution densities of Carslaw et al.¹⁰ The γ measured here at these [HCl] are a factor of 2–3 larger than the measurements of Elrod et al. ([HCl] was determined using the measured p_{HCl} and H^*_{HCl} from eq 19; there could be additional uncertainty introduced due to the uncertainty, $\sim 25\%$, in H^*_{HCl}). The good agreement with Hanson and Ravishankara² that they report (see their Figure 5) was apparently due to their extrapolation procedure; their comparison was complicated by a conversion from H_2SO_4 content to equivalent atmospheric temperature. Zhang et al. report γ for ClONO_2 in the presence of $\sim 4 \times 10^{-7}$ Torr of HCl. The Carslaw et al.¹⁰ model was used to assign H_2SO_4 content from the reported conditions, and H^*_{HCl} was taken from eq 19. The data of Zhang et al.⁶ are within 30% of the present results.

$\text{HNO}_3/\text{H}_2\text{SO}_4/\text{H}_2\text{O}$ Solutions. As can be seen in Figure 9, the results presented here suggest that γ_{R1} and γ_{R2} are significantly affected by the presence of HNO_3 . The $\gamma_{R1/R2}$ for B–D are $\sim 50\%$ lower than what would be expected for the equivalent water activity $\text{H}_2\text{SO}_4/\text{H}_2\text{O}$ solutions. For solution A (4 wt % HNO_3), the measured γ are close to those predicted for 48.2 wt % H_2SO_4 except for the HCl-free solution.

It is likely that HNO_3 perturbs both the bulk and the surface reaction terms. The solid and dashed lines in Figure 9 are the γ for case I and a modified case I, respectively. In the modified case the bulk term was divided by a factor of 2 in each case. Γ_s was unchanged for A, divided by two for B and C, and divided by 10 for D. The agreement between this crude approach and the measurements suggests that as liquid $[\text{HNO}_3]$ increases the surface reaction term decreases greatly while the effect on the bulk reactions does not seem to depend on $[\text{HNO}_3]$. A decreasing Γ_s could be explained by a decreasing surface excess of HCl and/or the surface equilibrium constant, b' , for ClONO_2 as HNO_3 increases.

The effect of HNO_3 on Γ_b , assuming it is as postulated above, is difficult to elucidate and probably cannot be explained by the effects of HNO_3 on only one parameter, i.e., H , k_{R1} , k_{R2} , or D_1 . Changes in D_1 are likely to be small because there is evidence that solution viscosity and thus D_1 will be largely unaffected by HNO_3 .^{31b} A possible explanation is that the decrease in Γ_b for solutions A and B is due to decreases in k_{R1} and k_{R2} when HNO_3 is present, meanwhile H is largely unaffected by these amounts of HNO_3 . Then as $[\text{HNO}_3]$ increases (solutions C and D) additional slowing of k_{R1} and/or k_{R2} is compensated for by an enhanced ClONO_2 solubility. A

TABLE 7: Comparison to Published Data for R2 for HNO₃/H₂SO₄/H₂O Solutions

T, K	H ₂ SO ₄ wt %	HNO ₃ wt %	γ (ref 5) ^a	γ (this work)	X ^b	γ _{R2} ^c
199	50.3	1.8	0.009 ± 0.001		0.165	0.019
196	36.4	11.2	0.032 ± 0.012		0.137	0.041
203	44.4	4.6		0.019 ± 0.004	0.146	0.033
204–5	39.6	7.9		0.022 ± 0.005	0.138	0.040
204.6	30	16.8		0.026 ± 0.006	0.131	0.048
205	20.3	25.6		0.042 ± 0.016	0.124	0.057

^a H₂SO₄ and HNO₃ contents assigned using Carslaw et al.¹⁰ ^b Mole fraction H₂SO₄ solution with the same *p*_{H₂O}.¹⁰ ^c Obtained from eq 11a, X for equivalent *a*_{H₂O} binary solution and γ_{R2} = (Γ_{R2}⁻¹ + 1)⁻¹.

slowing of the hydrolysis rate would be consistent with recent theoretical calculations by Bianco and Hynes⁴⁵ for the mechanism of ClONO₂ hydrolysis on water ice that involves proton transfer in a cyclic complex of ClONO₂ with three water molecules. They suggest that the presence of HNO₃/NO₃⁻ could interfere with the proton transfer and substantially decrease the hydrolysis rate.

In Tables 6 and 7 are presented comparisons of the present results with results from previous studies^{6,7} for HNO₃/H₂SO₄/H₂O solutions. The data of Elrod et al.⁷ suggest differences between γ_{R1} on HNO₃-free and HNO₃-doped solutions of -5 to -32% (on average -13%) with no apparent dependence on [HNO₃]. A rough comparison indicates there are differences of factors of 2–3 between the Elrod et al. measurements and the present results, about the same discrepancy noted above for the HNO₃-free solutions. Zhang et al.⁶ reported one measurement of γ_{R1} on a solution containing HNO₃, a 53 wt % H₂SO₄/1.2 wt % HNO₃ solution, calculated from the experimental conditions using the Carslaw et al.¹⁰ model. This amount of HNO₃ might not significantly affect the γ for ClONO₂, thus, their conclusion that γ_{R1} is not affected by HNO₃ was drawn from insufficient data. Zhang et al.⁶ also report that γ_{R2} is not affected by the presence of HNO₃ in the liquid. Note that, for the measurements where appreciable amounts of HNO₃ were present, their data are consistent (within the uncertainties) with a significant effect (compare their measured γ_{R2} with that predicted using eq 11a in Table 7). The *H*^{*_{HCl}} for the HNO₃/H₂SO₄/H₂O solutions extracted from the data presented in Table 5 are about 1/2 of the values from the Carslaw et al.¹⁰ model. Therefore, for solutions with acid content near to (or with equivalent water activity to) 45 wt % H₂SO₄, the current measured *H*^{*_{HCl}} are approximately 1/2 of the values from the Carslaw model. The predictions of Luo et al.²⁹ for the HNO₃/H₂SO₄/H₂O solutions are in quite good agreement with the measurements (Table 5), in general within 20% of the *H*^{*_{HCl}} reported here.

Alternative Fits of γ vs *p*_{HCl}. Two alternative parametrizations in the global fits to the data were tried. In case II, the expression for *k*_{R2} as discussed above (eq 11c) was used and *B*_{rel}(*X*) was taken to be proportional to *H* (eq 11b) divided by 10³. This approach contains the assumption that, in the absence of reaction, the amount of surface adsorbed ClONO₂ would be proportional to the amount of bulk adsorbed ClONO₂, the proportionality constant being independent of *X*. In this case, with

$$B_{\text{rel}}(X) = 10^{0.479-3.906X} \quad (21a)$$

values of the fitted parameters

$$a_0 = 1.54 \times 10^7 \text{ M}^{-1} \text{ s}^{-1} \quad b_0 = 55.7 \text{ M}^{-1} \quad (21b)$$

were obtained.

TABLE 8: Calculation of γ_{R1} and γ_{R2}^a

param or function	value or expression	note and ref
<i>X</i>	function of <i>p</i> _{H₂O} and <i>T</i>	eq 10 of Carslaw et al. ⁴⁶
Γ _{R2}	exp(-0.393 - 13.13 <i>X</i> - 50.914 <i>X</i> ²)	eq 11a
[HCl]	<i>H</i> ^{*_{HCl}} <i>p</i> _{HCl}	<i>H</i> ^{*_{HCl}} from eq 19
Γ _S	<i>b</i> ₀ <i>B</i> _{rel} [HCl]	<i>B</i> _{rel} = <i>a</i> _{H₂O} from (17a) ^b
<i>k</i> _{R1}	<i>a</i> ₀ <i>D</i> _{rel} [HCl]	<i>D</i> _{rel} (eq 16b) ^b
Γ _b	Γ _{R2} (1 + <i>k</i> _{R1} / <i>k</i> _{R2}) ^{0.5}	<i>k</i> _{R2} (eq 11c) ^b
<i>l</i>	(<i>D</i> /(<i>k</i> _{R1} + <i>k</i> _{R2})) ^{0.5}	<i>D</i> ₁ (eq 16a)
<i>f</i> (<i>r</i> / <i>l</i>)	coth(<i>r</i> / <i>l</i>) - <i>l</i> / <i>r</i>	<i>r</i> , particle radius
Γ _b '	<i>f</i> (<i>r</i> / <i>l</i>)Γ _B SA/(<i>f</i> (<i>r</i> / <i>l</i>)Γ _B + SA)	SA = <i>S</i> <i>k</i> _{sol} / <i>k</i> _{des} = 10
γ	1/(1/ <i>S</i> + 1/(Γ _b ' + Γ _S))	γ = γ _{R1+R2} ; <i>S</i> = 1
γ _{R1}	γ(Γ _S + Γ _b ' <i>k</i> _{R1} /(<i>k</i> _{R1} + <i>k</i> _{R2}))/(Γ _S + Γ _b)	
γ _{R2}	γ - γ _{R1}	

^a Inputs: *r* (particle radius, cm), *p*_{H₂O} and *p*_{HCl} (atm), *T* (K). Use of these expressions for temperatures outside of the range 190–215 K should be carefully considered. Also, special care should be taken when partial pressure of ClONO₂ is greater than that of HCl. ^b For case I, *a*₀ = 1.69 × 10⁷ and *b*₀ = 256.8 (eq 18). The values of *a*₀, *b*₀, *B*_{rel}, and *k*_{R2} for cases II and III are discussed in the text (eqs 21a,b and 22a–c).

In case III, *k*_{R2} was assumed to be proportional to water activity, *a*_{H₂O}, and the resulting *H* for ClONO₂ was calculated as described above. The activity of water was used as expressed in eq 17a and

$$k_{R2} = 8130a_{\text{H}_2\text{O}} \quad (22a)$$

to result in a value of ~600 s⁻¹ for 60 wt % H₂SO₄ (*X* = 0.216) at 203 K. A least-squares fit to the resulting *H* values yields *H* = 10^{4.256-7.415*X*}. Fitting the data shown in Figure 8a assuming *B*_{rel} was proportional to this *H* resulted in poor fits: the value *a*₀ was 0 ± 1 × 10⁶ M⁻¹ s⁻¹, indicating nonsensically that there is no bulk reaction. Therefore, the quantity

$$B_{\text{rel}}(X)b_0 = b'_0 + b'_1X \quad (22b)$$

was tried and satisfactory fits were obtained resulting in the values

$$a_0 = 7.71 \times 10^6 \text{ M}^{-1} \text{ s}^{-1} \quad b'_0 = 44.38 \text{ M}^{-1} \\ b'_1 = -66.124 \text{ M}^{-1} \quad (22c)$$

In general, cases II and III fit the data as well as case I above. However, in the solutions where γ_{R1} is most important, 45 and 49.5 wt %, case I represents the measured γ best. The differences in the γ predicted for atmospheric conditions by these cases are small and are discussed below.

Stratospheric Conditions. Shown in Table 8 are the equations 13–19 used to calculate γ_{R1} and γ_{R2} for atmospheric conditions. Mole fraction of H₂SO₄ can be calculated from *p*_{H₂O} and temperature using an expression presented by Carslaw et al.⁴⁶ Shown in Figure 11 are the reaction probabilities for R1 and R2 for typical cold lower stratospheric conditions (*p*_{H₂O} = 2.63 × 10⁻⁷ atm, *p*_{HCl} = 1 × 10⁻¹⁰ atm, 190 K < *T* < 215 K) from the previous formulation² (referred to as HR94) and those from this work (Table 8; cases I–III). *S* (for eq 13) and α (for ref 2) were taken to be unity. In general, the calculated reaction probabilities for R1 from HR94 are in good agreement with those presented here. At low temperatures, case I γ_{R1} are 10–20% less than HR94 and γ_{R1} for cases II and III are in turn 10–20% less than case I. γ_{R2} for cases I and II are nearly identical and are significantly larger than HR94 for *T* < 205 K (*X* < 0.25). This is due to three effects: slightly larger Γ_{R2}

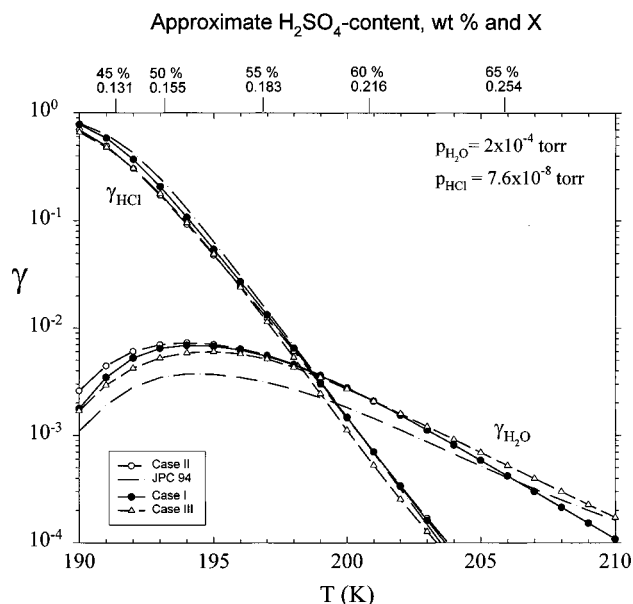


Figure 11. γ_{R1} and γ_{R2} are plotted as a function of temperature for typical stratospheric conditions of $p_{\text{H}_2\text{O}} = 2.63 \times 10^{-7}$ atm, $p_{\text{HCl}} = 1 \times 10^{-10}$ atm, and particle radius = 1×10^{-5} cm. Filled (case I) and open (case II) circles and triangles (case III) are results of this work (Table 8), and the dash-dot lines are from Hanson and Ravishankara.² The H_2SO_4 content is indicated at the top of the plot. Note that the absorption of HNO_3 was not taken into account and γ will be appreciably affected below 192 K.

than γ_0 of HR94, differences in reacto-diffusive lengths, and a smaller surface reaction term here. Less competition with the HCl surface reaction results in a larger contribution from bulk HCl and H_2O reactions. γ_{R2} for case III in particles varies with H_2SO_4 content differently than cases I and II. This is in part due to different reacto-diffusive lengths predicted for the two different k_{R2} formulations. As mentioned above, measurements of l for a variety of H_2SO_4 contents would help to determine the variation of k_{R2} with X . These differences are probably not consequential to atmospheric modeling calculations. Note that case I best fits the data for solutions where R1 is most important (45 and 49.5 wt %) and for this reason is preferred.

For the calculation of γ as a function of atmospheric conditions (T , $p_{\text{H}_2\text{O}}$, p_{HCl} , etc.), eqs 13–19 will give accurate values (i.e., representative of the measurements) within a limited range of temperature. It is likely this range includes the stratospherically important temperatures 190–215 K, which are within ± 10 K of the measurements, because the γ for a given [HCl] are essentially temperature independent over this range. The γ are determined to a large extent by HCl content, and the H^*_{HCl} given by eq 19 varies with temperature in accord with the data and models.^{10,29,37} The γ were measured to an accuracy of ± 15 –25% over solutions with [HCl] that cover the range expected in the stratosphere, with the exception of the 45 wt % H_2SO_4 solutions where γ could not be measured accurately for stratospheric [HCl]. The uncertainties in the fitted parameters, for case I for example, $\sigma_{a_0}/a_0 = 17\%$ and $\sigma_{b_0}/b_0 = 13\%$, are comparable to the measurement uncertainty. Thus the accuracy of the calculated γ is likely to be on the order of the uncertainty in the measured γ . Error due to the uncertainty in the temperature dependence of H^*_{HCl} (± 0.5 kcal mol⁻¹ in solvation enthalpy, estimated by comparing eq 19 and the data to the models^{10,29,37}) results in additional uncertainty of up to 10% for $T = 190$ K. The overall uncertainty in the calculated γ is estimated to be $\pm 30\%$.

The incorporation of HNO_3 into the particles was not taken

into account in Figure 11. From the results shown in Figure 9, a large effect is expected when [HNO₃] is larger than ~ 5 wt %. [HCl] levels expected in the lower stratosphere for solutions B–D are 4×10^{-3} , 9×10^{-3} , and 2×10^{-2} M, respectively (for $p_{\text{HCl}} = 1 \times 10^{-10}$ atm and assuming an exponential temperature dependence, specifically $\exp(5500/T)$, to the H^*_{HCl} measured here, Table 5). By extrapolation of the dashed lines in Figure 9 to these [HCl], $\gamma = 0.19$, 0.34, and 0.30 for solutions B–D, respectively. These are decreases of 40, 33, and 57%, respectively, from that predicted for the corresponding HNO_3 free solutions. The effect of dissolved HNO_3 on γ for ClONO_2 is significant and should be investigated further in the laboratory and also considered in atmospheric modeling calculations.

Summary

The reaction probabilities for ClONO_2 due to hydrolysis and reaction with HCl measured here supplement previous work from this laboratory.² The HCl solubility measurements presented here and those of Elrod et al.,⁷ in conjunction with the detailed model calculations of Carslaw et al.¹⁰ and Luo et al.,²⁹ provide a firm basis for calculating the HCl content of cold, stratospheric sulfuric acid aerosol. The mole fraction based parametrization for calculating γ applicable to the atmosphere presented here is in good agreement with a previous model using a water activity based description.²

The variation of the measured reaction probabilities with HCl reveal there is a significant contribution from a surface reaction between ClONO_2 and HCl. A significant effect on γ for R1 and R2 due to the presence of HNO_3 dissolved in sulfuric acid solutions was also found, particularly on the surface-specific reaction. Measurements on small sulfuric acid particles indicate a lower limit to the sticking coefficient of ClONO_2 of 0.5. It was shown that these measurements are consistent with a value for S close to unity.

To address some of the issues raised here, measurements of ClONO_2 hydrolysis as a function of particle size (i.e., to obtain the reacto-diffusive length) for a range of sulfuric acid contents are planned. Also, more extensive measurements of R1 at temperatures other than 203 K would help to precisely discern the small temperature dependence of this reaction. More measurements of ClONO_2 loss on $\text{HNO}_3/\text{H}_2\text{SO}_4/\text{H}_2\text{O}$ solutions are needed to further understand the effect of HNO_3 on γ for ClONO_2 . The effect of dissolved HNO_3 on the reacto-diffusive length will help to determine if the k_{R2} (or k_{R1}) are decreased due to HNO_3 .

Acknowledgment. Conversations with L. G. Huey, E. R. Lovejoy, C. A. Longfellow, and A. R. Ravishankara are gratefully acknowledged. The comments of the reviewers were greatly appreciated. This work was in part supported by NOAA's Climate and Global Change program. A text file containing the equations presented in Table 8 is available (e-mail: dhanson@al.noaa.gov).

References and Notes

- (1) WMO, Scientific assessment of ozone depletion: 1991, WMO Report No. 25, 1991.
- (2) Hanson, D. R.; Ravishankara, A. R. *J. Phys. Chem.* **1994**, *98*, 5728.
- (3) (a) Tolbert, M. A.; Rossi, M. J.; Golden, D. M. *Geophys. Res. Lett.* **1988**, *15*, 847. (b) Rossi, M. J.; Malhotra, R.; Golden, D. M. *Geophys. Res. Lett.* **1987**, *14*, 127. (c) Williams, L. R.; Manion, J. A.; Golden, D. M.; Tolbert, M. A. *J. Appl. Meteor.* **1994**, *33*, 785.
- (4) Hanson, D. R.; Ravishankara, A. R. *J. Geophys. Res.* **1991**, *96*, 17307.
- (5) Zhang, R.; Leu, M.-T.; Keyser, L. *Geophys. Res. Lett.* **1995**, *22*, 1493.

- (6) Zhang, R.; Leu, M.-T.; Keyser, L. *J. Phys. Chem.* **1994**, *98*, 13563.
- (7) Elrod, M. J.; Koch, R. E.; Kim, J. E.; Molina, M. J. *Faraday Discuss.* **1995**, *100*, 269.
- (8) Robinson, G. N.; et al. *J. Geophys. Res.* **1997**, *102*, 3583.
- (9) Ravishankara, A. R.; Hanson, D. R. *J. Geophys. Res.* **1996**, *101*, 3885.
- (10) Carslaw, K. S.; Clegg, S. L.; Brimblecombe, P. *J. Phys. Chem.* **1995**, *99*, 11557.
- (11) Tabazadeh, A.; Toon, O. B.; Clegg, S. L.; Hamill, P. *Geophys. Res. Lett.* **1997**, *15*, 1931.
- (12) Carslaw, K. S.; et al. *Geophys. Res. Lett.* **1994**, *21*, 2479–2482.
- (13) (a) Tabazadeh, A.; Turco, R. P.; Jacobson, M. Z. *J. Geophys. Res.* **1994**, *99*, 12897. (b) Drdla, K.; et al. *Geophys. Res. Lett.* **1994**, *21*, 2475.
- (14) Beyer, K. D.; Seago, S. W.; Chang, H. Y.; Molina, M. J. *Geophys. Res. Lett.* **1994**, *21*, 871.
- (15) Danckwerts, P. V. *Gas-liquid reactions*; McGraw-Hill: New York, 1970.
- (16) Hanson, D. R. *J. Phys. Chem. B* **1997**, *101*, 4998. For measurements on particles of radius a , the Γ_b term is multiplied by: $\coth(a/l) - l/a$, where $l \equiv (D_1/k)^{1/2}$ is the reacto-diffusive length.
- (17) Lovejoy, E. R.; Huey, L. G.; Hanson, D. R. *J. Geophys. Res.* **1995**, *100*, 18775.
- (18) Hanson, D. R.; Lovejoy, E. R. *J. Phys. Chem.* **1996**, *100*, 6397.
- (19) Hanson, D. R.; Ravishankara, A. R. *J. Geophys. Res.* **1991**, *96*, 5081.
- (20) Huey, L. G.; Hanson, D. R.; Howard, C. J. *J. Phys. Chem.* **1995**, *99*, 5001.
- (21) Giauque, W. F.; Hornung, E. W.; Kunzler, J. E.; Rubin, T. R. *J. Am. Chem. Soc.* **1960**, *82*, 62. The H₂O vapor pressures of H₂SO₄ solutions given by this work are in excellent agreement with those of Carslaw et al.¹⁰ After most of the experiments, samples of the acid solutions were titrated with standardized NaOH solutions to determine H₂SO₄ content (typical accuracy of ± 0.5 wt %). The H₂SO₄ content was within ± 0.7 wt % of that determined by $p_{\text{H}_2\text{O}}$ and temperature. For more details on water vapor in these types of experiments, see note 23 of ref 18.
- (22) (a) Brown, R. L. *J. Res. Natl. Bur. Stand. (U.S.)* **1978**, *83*, 1. (b) Motz, H.; Wise, H. J. *J. Phys. Chem.* **1960**, *32*, 1893. (c) Howard, C. J. *J. Phys. Chem.* **1979**, *83*, 3.
- (23) For example, a small amount of reagent 38 wt % HCl solution (0.062 g) was mixed with 29.4 g of precooled (273 K) 45 wt % H₂SO₄ resulting in a ~ 44.9 wt % H₂SO₄ solution containing 0.079 wt % HCl. A small portion of this was diluted with 45 wt % H₂SO₄ to obtain 5.3×10^{-5} wt fraction HCl (equal to 2×10^{-3} M for a density of 1.41 g cm⁻³ at 202.5 K).¹⁰
- (24) Hanson, D. R.; Ravishankara, A. R. *J. Phys. Chem.* **1993**, *97*, 12309.
- (25) Lovejoy, E. R.; Hanson, D. R. *J. Phys. Chem.* **1995**, *99*, 2080.
- (26) (a) Mason, E. A.; Monchick, L. *J. Phys. Chem.* **1961**, *36*, 2746. (b) Patrick, R.; Golden, D. M. *Int. J. Chem. Kinet.* **1983**, *15*, 1189.
- (27) Lovejoy, E. R. Ph.D. Thesis, Department of Chemistry, University of Colorado, Boulder, Co, 1988.
- (28) A detailed description of a flowing afterglow CIMS apparatus is given by: Ferguson, E. E.; Fehsenfeld, F. C.; Schmeltekopf, A. L. *Adv. At. Mol. Phys.* **1969**, *5*, 1. Equation 6a can be shown to be equivalent to eq 5 with the equations $dS'_{162} = k_{162} n_{\text{HCl}} S'_{146}$ and $n_{\text{HCl}} = F_{\text{HCl}} L_0 / V_F$, where n_{HCl} is the HCl number concentration in the CIMS, and making the identity that $S'_{162} = dS'_{162}$ and $t = dt$ (valid for $S'_{162}/S'_{146} \ll 1$).
- (29) Luo, B. P.; Carslaw, K. S.; Peter, T.; Clegg, S. L. *Geophys. Res. Lett.* **1995**, *22*, 247.
- (30) In this work, the ³⁴SF₆⁻ isotope (148 amu) was monitored to avoid additional errors due to "rolloff" (due primarily to a ~ 2 MHz preamplifier) corrections to the high count rate 146 amu peak. In the previous work,²⁴ the ³²SF₆⁻ signal was used, and a simple correction factor, $1 + S_{146}/2$ MHz was used. Three previous data points for H^*_{HCl} measurements over 45 wt % H₂SO₄ were not included because the CIMS HCl calibration data for these measurements could not be located.
- (31) (a) Williams, L.; Golden, D. M. *Geophys. Res. Lett.* **1993**, *20*, 2227. (b) Williams, L. R.; Long, F. S. *J. Phys. Chem.* **1995**, *99*, 3748.
- (32) The D_1 for ClONO₂ were taken to be those of HOCl: Huthwelker, T.; Peter, Th.; Luo, B. P.; Clegg, S. L.; Carslaw, K.; Brimblecombe, P. *J. Atmos. Chem.* **1995**, *21*, 81. This calculation was shown to be accurate for HOCl diffusion in 60 wt % H₂SO₄ at 250 K.¹⁸
- (33) Solubility for HOCl taken from: Donaldson, D. J.; Ravishankara, A. R.; Hanson, D. R. *J. Phys. Chem. A* **1997**, *101*, 4717. Donaldson et al. presents a slight revision to the calculated H_{HOCl} of Huthwelker et al.³² in solutions containing 60 wt % H₂SO₄ or greater ($X > 0.22$). Donaldson et al. pointed out the importance of ensuring pseudo-first-order conditions in the liquid. Here, [ClONO₂] is less than 10^{-6} M for all solutions ($p_{\text{ClONO}_2} \leq 3 \times 10^{-10}$ and $H \leq 10^3$ M/atm), which is much less than the [HCl] when R1 was studied.
- (34) Hanson, D. R.; Lovejoy, E. R. *Science* **1995**, *267*, 1326. These authors also presented arguments that l in 60 wt % H₂SO₄ is nearly temperature independent.
- (35) Table 3 of ref 8 contains a few errors: the Γ_i should be equal to $\exp(-S_{\text{HOCl}} n_{\text{H}_2\text{SO}_4})$, with $S_{\text{HOCl}} = -0.04107 + 54.56/T$ (see ref 32). The lines shown in Figure 6 were calculated as in Table 3 of ref 8 with these corrections. A close examination of the parameters for 60 wt % H₂SO₄ between 190 and 260 K reveals inconsistencies in the Robinson et al. work. The values shown in Figure 4⁸ are not equal to the Table 3⁸ calculations, and there is a distinctly different temperature dependence. The D_1 given by their expression is between a factor of 0.25 and 0.05 of those of refs 31 and 32 and about 20–70% less than those shown in their Figure 7c. There appear to be large discrepancies between the Robinson et al. parametrization of the viscosity of sulfuric acid solutions given in their Table 3 and the measured values.^{31b} The H^* and k_{rxn} given in Table 3⁸ are equal to the values shown in Figure 9;⁸ using the D_1 shown in Figure 7c⁸ results in γ_{R2} up to 70% greater than those shown in Figure 4.⁸
- (36) Zhang, R.; Wooldridge, P.; Molina, M. J. *J. Phys. Chem.* **1993**, *97*, 8541.
- (37) Tabazadeh, A.; Turco, R. P.; Jacobson, M. J. *J. Geophys. Res.* **1994**, *99*, 12897.
- (38) In addition, time-dependent uptake measurements in a flow tube apparatus²⁴ are probably not as accurate as those performed in a Knudsen-cell type apparatus^{31a} and should use a more involved analysis procedure to obtain $H^*_{\text{HCl}} D_1^{0.5}$. Simulations of the flow tube experiments²⁴ by T. Huthwelker (private communication, 1995) showed that values for $H^*_{\text{HCl}} D_1^{0.5}$ are about 25% higher than that obtained from the simple analysis.^{15,24,31a}
- (39) Hanson, D. R.; Mauersberger, K. *Geophys. Res. Lett.* **1988**, *15*, 855. $p_{\text{H}_2\text{O}}$ was not measured here (only a relative measure was performed for solution D, before vs after freezing). If the absolute value of $p_{\text{H}_2\text{O}}$ is 20% less than that given by the Carslaw et al. model,¹⁰ p_{HNO_3} over NAT would be 75% greater. This, combined with the uncertainty in the measured p_{HNO_3} , $\pm 35\%$, makes agreement to a factor of 2 satisfactory.
- (40) Hanson, D. R.; Ravishankara, A. R. *J. Geophys. Res.* **1993**, *98*, 22931.
- (41) In a footnote in ref 34, it was assumed that the surface specific reaction term did not contribute more than 15% to the γ_{R1} measured in 60 wt % H₂SO₄ at 250 K. If this is true, a decrease in b_0 of about 60% or greater is implied on going from 203 to 250 K.
- (42) The extrapolation of measured viscosities to low temperatures is problematic; values extrapolated 10 K outside the measurement temperatures, using the equation of Williams and Long,^{31b} are up to a factor of 5 larger than the highest measured values. The viscosity relation presented by Robinson et al.⁸ has a steeper T -dependence than the Williams and Long equation (see note 35); using the Williams and Long equation to extrapolate D_1 results in predicted decreases in γ_{R2} of only 5–12% from 202 to 190 K. Eicher and Zwolinski (*J. Phys. Chem.* **1971**, *75*, 2016) warned against the use of this type of equation to extrapolate viscosity data outside the experimental temperature range.
- (43) Hanson, D. R. *J. Phys. Chem.* **1995**, *99*, 13059.
- (44) Note that $a_{\text{H}_2\text{O}}$, D_1 , and k_{R2} are functions of X . D_1 varies with X in approximately the same way as $a_{\text{H}_2\text{O}}$ (eqs 16 and 18); the relative variation is at most a factor of 2 (compare D_1 and $a_{\text{H}_2\text{O}}/10^7$) over the range 40–75 wt % H₂SO₄. As k_{R2} is proportional to the square of $a_{\text{H}_2\text{O}}$ for case I, the calculated ρ (eq 20) will vary a factor of 2 depending upon what composition is chosen.
- (45) Bianco, R.; Hines, J. T. *J. Phys. Chem. A* **1998**, *102*, 309.
- (46) Carslaw, K. S.; Luo, B.; Peter, T. *Geophys. Res. Lett.* **1995**, *22*, 1877.